WT-1475

AEC Category: HEALTH AND SAFETY
Military Category: 72

OPERATION PLUMBBOB

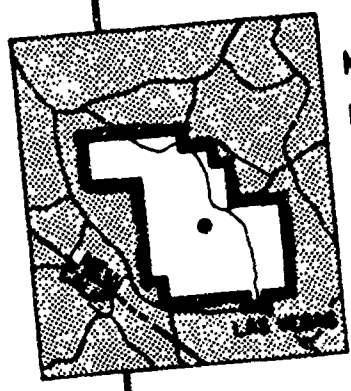

NEVADA TEST SITE
MAY-OCTOBER 1957

Project 34.4

BLAST EFFECTS ON AN AIR-CLEANING SYSTEM

Issuance Date: October 22, 1962

CIVIL EFFECTS TEST GROUP

Report to the Test Director

BLAST EFFECTS ON AN AIR-CLEANING SYSTEM

By

Richard Dennis
Charles E. Billings
Leslie Silverman

Approved by: L. J. VORTMAN
Director
Program 34

Approved by: L. J. DEAL
Acting Chief
Civil Effects Branch

Harvard University Air Cleaning Laboratory
Boston, Massachusetts
April 1962

NOTICE

This report is published in the interest of providing information which may prove of value to the reader in his study of effects data derived principally from nuclear weapons tests.

This document is based on information available at the time of preparation which may have subsequently been expanded and re-evaluated. Also, in preparing this report for publication, some classified material may have been removed. Users are cautioned to avoid interpretations and conclusions based on unknown or incomplete data.

PRINTED IN USA
[redacted]. Available from the Office of
Technical Services, Department of Commerce,
Washington 25, D. C.

USAEC Division of Technical Information Extension, Oak Ridge, Tennessee

ABSTRACT

Objectives of this project were (1) to determine the effects of blasts on filtration devices and typical gas-cleaning systems in the 3- and 1-psi overpressure range, (2) to measure dust dislodged from AEC filters and dry plates by blast and reentrained in reverse-flow air, (3) to determine the pressure attenuation and dust-recovery characteristics of typical wire-mesh viscous filters and dry Fiberglas filters, (4) to determine the natural damping effect of duct work and stacks, and (5) to compare field and laboratory data to determine if present and future laboratory tests can be extrapolated to predict field conditions.

Test results showed no damage to AEC filters and only minor damage to Fiberglas filters. Total reentrainment ranged from 73 per cent of total AEC filter loading (4.0-psig area) to 53 per cent (1.9-psig area). Dry plates lost 95 per cent of their original dust holding. Prefilters recovered approximately 30 per cent of the dust dislodged from AEC filters. Wire-mesh after-filters reduced dust loss from 53 to 4.5 per cent. Field tests appear to agree with laboratory studies and indicate that future tests can be performed successfully in laboratory shock tubes.

ACKNOWLEDGMENTS

The authors wish to thank Luke J. Vortman, Director of Program 34, for his technical and administrative assistance; Robert A. Cameron and Robert A. Williamson, Program 34, for their field assistance in installing test apparatus; and Edwin Bryant of the Ballistic Research Laboratories for his field support in providing pressure–time instrumentation.

CONTENTS

CONTENTS (Continued)

ILLUSTRATIONS

ILLUSTRATIONS (Continued)

TABLES

Chapter 1

INTRODUCTION

1.1 PRIMARY OBJECTIVES

At the request of the Division of Reactor Development, U. S. Atomic Energy Commission, a study of the effect of shock waves on various types of air-cleaning equipment has been undertaken by the Harvard University Air Cleaning Laboratory. This investigation is concerned specifically with shock waves generated by nuclear or high-explosive blasts which impact upon air-cleaning devices in a direction opposite to that of normal air flow. Major blast effects under investigation are destruction or damage to air-cleaning equipment designed to collect radioactive materials and dislodgement and subsequent reentrainment (resuspension in the air) of radioactive dust from collector surfaces by the reverse air flow produced by the blast. Reentrainment alone is a serious problem even without physical damage to air-cleaning devices since there is a possibility of contaminating plant process and laboratory areas with highly radioactive materials.

Air-cleaning equipment used for the final removal of radioactive materials from stack effluents must be very efficient (>99.9 per cent) to prevent contamination of in- and out-plant atmospheres by fission products arising from concentration, extraction, metallurgical treatment, or fabrication of radioactive substances. Depending upon the amount and nature of dust filtered from the gas stream, the dust deposit on, or near, the surface of the air-cleaning device may be highly radioactive. The impact of a shock wave upon the downstream face of a filter will dislodge this dust from the upstream or collecting surface of the unit. The reverse air flow accompanying the shock will reentrain part of this dust; and, depending upon the intensity and duration of the shock wave, it may blow the dust back through the ventilation system to the areas from which it came. Resulting general contamination would seriously hamper, if not halt indefinitely, plant operations in these areas.

Not only blast characteristics per se but also structural geometry and quantity, physical state, and activity level of the dust itself influence the magnitude of the contamination problem likely to arise from reentrainment. Although blast valves might serve to minimize dust reentrainment, and thus eliminate damage to air-cleaning apparatus, they are not commonly employed at AEC sites primarily because of the technical problems involved. Therefore investigation of them does not fall within the scope of this study.

Primary objectives of this study are: (1) to determine the nature and extent of structural damage to ductwork systems and filtration apparatus, (2) to determine the amount of dust dislodged and reentrained from normal collecting surfaces of air-cleaning devices and connecting ductwork, (3) to determine how structural damage may be prevented or significantly reduced, and (4) to determine how reentrainment may be prevented or reduced if no serious structural damage occurs.

1.2 REVIEW OF LABORATORY RESULTS

Achievement of these objectives ultimately depends upon both laboratory and field tests since there is a definite limit to the extent to which laboratory tests can simulate actual blast effects. However, preliminary laboratory shock-tube tests have provided a convenient and economical means of establishing damage pressure levels and of estimating the amount of dust reentrainment. A description of laboratory apparatus and a discussion of experimental results have been reported by Billings et al.[1] Typical results of this study are summarized in Table 1.1.

TABLE 1.1—SUMMARY OF SHOCK-TUBE FILTER TESTS

Filter type*	Shock pressure, psi	Duration of positive phase,† msec	Total impulse,‡ psi-msec	Initial filter loading, g	Dust loss, g	Calculated equivalent nuclear explosion§		Effects
						Distance, ft	Yield, kt	
D	0.5							Moderate damage
D	1.5							Complete failure
AEC-6	2.1	720	605			4800	3.5	No damage
AEC-6	3.1	860	1070			5600	14	Partial failure
AEC-6	6.0	860	2060			5200	30	Complete failure
AEC-6	1.7	660	430	155	152	6500	7	98% dust removal
AEC-6	1.9	850	650	26	8	7600	13	32% dust removal
AEC-12	2.5	790	790	429	359	6800	13	84% dust removal
AEC-12	2.4	760	730	39	20	5350	8	51% dust removal

*D is a Dust-Stop Fiberglas filter (20 by 20 by 2 in., 800 cu ft/min rated capacity), AEC-6 is a pleated-paper filter (24 by 24 by 6 in., 500 cu ft/min rated capacity), and AEC-12 is a pleated-paper filter (24 by 24 by 12 in., 1000 cu ft/min rated capacity).

†No negative-pressure phase observed.

‡Summation of area under pressure–time curve.

§Based upon unpublished data of Sandia Corporation.

It appears from these tests that Dust-Stop cardboard-frame Fiberglas-packed prefilters experience moderate damage at shock overpressures of 0.5 psi and severe damage at pressures greater than 1.5 psi. Pleated AEC absolute type high-efficiency filters sustain moderate damage at 3.0 psi and are completely destroyed at overpressures greater than 5.0 psi. Pressure levels less than 2.5 psi caused no obvious physical damage although resistance to air flow in some cases appeared slightly lower than preshock values.

Reentrainment studies indicated that large amounts of dust were dislodged from AEC filters by shock overpressures ranging from 1.7 to 2.5 psi. Average dust loss for fully loaded filters amounted to 90 per cent of the initial dust holding in contrast to a 40 per cent loss for partially loaded filters. A fully loaded filter is defined as one containing sufficient dust to increase its resistance to air flow to twice its initial or clean value.

Equivalent high-explosive yields and theoretical distances of the filter from such blasts have been calculated from observed peak pressure and total impulse imparted to the filter. In general, laboratory shock tests appear to have simulated nuclear blasts equivalent to yields of 3.5 to 30 kt at distances of from 4800 to 7600 ft. Although extrapolation to field conditions may be subject to error (see Sec. 1.3), a preliminary examination shows values to be in the expected order of magnitude.

1.3 SIGNIFICANCE OF LABORATORY STUDIES

Two major conclusions can be drawn from laboratory findings. First, shock waves producing pressures greater than 2.5 psi upon downstream faces of AEC type filters will render the filter unfit for future use (except for immediate emergency purposes). Second, even when no apparent physical damage occurs (2-psi range), large quantities of dust may be dislodged from the filtering surfaces and projected back through the ventilation system. Although no laboratory data are available to correlate dust dislodgement with overpressure, it is believed that a reentrainment problem may exist at much lower pressures than those investigated in the laboratory. This applies specifically to windowless concrete structures wherein the only point of shock-wave entry is through the exhaust or supply ventilation ports. It is possible that stack and duct systems, normally located downstream of the air-cleaning devices, might serve to attenuate external pressure conditions so that nondamaging shocks would impact upon filtration equipment. Since space limitations did not permit pressure-attenuation studies in the laboratory, it is important that they be investigated in the field on prototype air-cleaning systems. Roughing or precleaning equipment should be included in both pressure-attenuation and dust-reentrainment studies since it is usually employed in typical filtration systems to extend the service life of high-efficiency filters.

1.4 EXTRAPOLATION LIMITS OF LABORATORY STUDIES

Although laboratory tests have furnished at least an order-of-magnitude answer to some of the items outlined in Sec. 1.1, space limitations and the resulting lack of geometric similarity with regard to field assemblies may not permit direct extrapolation of these findings to field experience. It is hoped that proper correlation between laboratory and field analytical methods and experimental results will permit continuation of the project on a laboratory scale.

The advantages of laboratory study are manifold: A shock tube is ready for use at any time; furthermore, a single tube may be employed to simulate a wide span of shock effects. To achieve comparable flexibility in the field, one test location and several blasts of varying intensity, or several locations and a single blast, are required. In the latter case, one must presume that predicted blast yield is reliable. If blast scheduling is contingent upon meteorology or on parallel experiments, tests may be prolonged.

Laboratory experiment planning may be altered immediately on the basis of a single test, whereas any miscalculation in field tests may incur lengthy time delays or invalidate the entire study.

Exclusive of the devices producing the blast, i.e., shock tube or nuclear weapon, approximately 10 times as much test equipment is required for field testing. Field assembly costs are estimated to be at least twice those for ordinary construction. Approximately one man-day is required for a single laboratory shock-tube test in contrast to an estimated five man-days for the equivalent field experiment. It appears that the cost advantage of laboratory tests exceeds that of field tests by at least a factor of 6; therefore successful correlation of laboratory and field events is considered an essential phase of this project.

1.4.1 Pressure–Time Relations

Laboratory tests were conducted in a 20-in.-diameter shock tube connected at the entry end to a 500-cu ft-capacity pressure chamber and vented at the opposite end to a plenum chamber. Test filters were supported in a special adapter section located 4 ft from the pressure-chamber exit. Shock waves were generated by the bursting of calibrated paper rupture diaphragms located in the shock-tube inlet. Pressure reflections were minimized within the shock tube by partitioning the plenum or venting chamber with cinder blocks and using a perforated Masonite-board wall.

Shock pressures were measured with a 1-in.-diameter diaphragm in the tube wall about 4 in. from the test filter. Pressure changes normal to the direction of the incident shock front were transmitted to a mechanically linked mirror which reflected a collimated light beam to a moving strip of photographic paper. Instrument frequency response was rather low (50 to 70

cycles) and the band width of the tracings was broad; therefore estimates of initial peak pressures and average pressures may have been only approximate. However, since basic operating principles of this device are the same as those employed with the Ballistic Research Laboratories (BRL) recorder (see Sec. 2.2), evaluation of the laboratory instrument is sought by comparison of field measurements obtained with the BRL device.

1.4.2 Duration of Positive-pressure Phase

The major factor limiting extrapolation of laboratory pressure–time data lies in the comparatively small air volume vented through the shock tube. For example, to reduce an initial chamber static pressure of 3.0 psi to ambient requires a release of only 100 cu ft of standard air. With no obstructions in the shock tube, static pressures recorded in the filter test location returned to atmospheric levels in less than 0.2 sec. On the other hand, field observations[2] have indicated that the positive-pressure period may last from 0.3 to 15 sec, depending on yield and distance from blast.

However, tests with high-resistance filters (AEC type) showed time durations in the range of 600 to 900 msec for the positive-pressure phase. Except for initial pressure, persistence in overpressure was caused by the relatively slow venting rate of the filter and not by continuance of true external shock conditions. For example, the air-flow rate through a 6-in. AEC filter is restricted to 800 cu ft/sec with an overpressure of 3 psi. As air is vented, static overpressure decreases, which, in turn, decreases air flow in such a way that 400 to 600 msec are required for pressure to return to ambient.

If blast effects upon a filter are measured in terms of peak overpressure and total impulse (as determined by integration of pressure–time curves), it appears that laboratory and field tests should be comparable insofar as high-resistance filters are concerned. However, damage to, and reentrainment from, low-resistance air cleaners, i.e., electrostatic precipitators or Fiberglas filters, may be greater under field conditions.

1.4.3 Pressure Equilibration

The comparatively small gas volume ejected from the shock tube into the plenum chamber did not cause significant change in ambient pressure; thus indicated overpressures always referred to background atmospheric levels (14.7 psi). An entirely different situation may exist under field conditions where the complete structure housing ventilation and air-cleaning equipment is subjected to shock pressures. If shock pressures are transmitted to the building interior other than through the stack system, the net force exerted upon filtration apparatus and the volume of reverse-flow air passing through the system may be reduced. Field studies should permit partial evaluation of this effect although it is realized that the type of building and the number and location of entry portals may produce considerable variation.

1.5 APPROACH TO FIELD TESTS

Project 34.4 tests are a continuation of laboratory studies described in Secs. 1.2 to 1.4. Their primary purpose was to determine effects of nuclear blasts upon air-cleaning systems under typical field conditions. Since the scope of the project was limited with respect to predictable overpressures and available structures, an important consideration in experiment design has been to simulate previous laboratory tests whenever possible. Under these conditions comparison of laboratory and field data should indicate whether or not small-scale laboratory tests afford a reliable approach to filter-damage and reentrainment studies.

The following field experiments have been designed:

1. Determination of pressure–time relations outside test buildings and immediately in front of air-cleaning devices undergoing damage-level tests.
2. Correlation of dust reentrainment from high-efficiency filters and low-voltage electrostatic precipitators with shock-wave intensity and duration.
3. Determination of the degree of pressure attenuation obtainable through the natural damping effect of a typical stack and ductwork system.

4. Evaluation of low-efficiency prefilters as pressure-attenuation devices when located either upstream or downstream of high-efficiency AEC filters.

5. Determination of effectiveness of precleaner filters in recovering dust dislodged from high-efficiency filters and electrostatic precipitators.

6. Comparison of field and laboratory pressure instrumentation.

REFERENCES

1. C. E. Billings, R. Dennis, and L. Silverman, Blast Damage to Air Cleaning Devices (Filter Tests), USAEC Report NYO-1595, Harvard Air Cleaning Laboratory, Nov. 28, 1955.
2. S. Glasstone (Ed.), "The Effects of Nuclear Weapons," p. 75, June 1957, Superintendent of Documents, U. S. Government Printing Office, Washington 25, D. C.

Chapter 2

PROCEDURE

2.1 TEST LOCATION AND STRUCTURES

Field tests were conducted in a chemical-plant control room and in a concrete house. Overpressures in these locations were expected to be about 3 and 1 psi, respectively.

The chemical plant control room is a one-room single-story steel-frame building with reinforced poured gypsum walls and roof. The over-all building dimensions are 26 by 22 by 11 ft high. Corrugated plastic panels originally located along the upper length of one wall were replaced by 4- by 4-in. wood beams to form a solid wall. All windows and doors were closed in by reinforced plywood panels. Grouting of cracks and seams restricted air entry for practical purposes to the ventilation stack extending through the building roof and to a single Dust-Stop filter housed in a 20- by 20-in. frame in the door.

The concrete house is a four-room residence type structure with attached garage. All windows and doors opening to the outside or to the garage were closed in with plywood and timbers. Except for the stack the only other opening to the building was a 20- by 20-in. Dust-Stop filter framed in the door leading to the garage. Dimensions, excluding garage, are approximately 29 by 27 by 8 ft high. Interior concrete walls were not altered except for openings required to install test apparatus. Cracks and seams were grouted to keep air infiltration as low as possible. Figures 2.1 and 2.2 are preshot photographs of the two structures which show the Dust-Stop filters mounted on the walls.

2.2 TEST APPARATUS

2.2.1 Ductwork and Hood Arrangement

Identical ventilation systems were constructed for the chemical-plant control room and the concrete residence. Figures 2.3 and 2.4 show plan views of this equipment in relation to building orientation. Although the ventilation systems were similar, it should be noted that the concrete house contained interior partitions, whereas the chemical-plant control room consisted of one large room. (See Fig. 2.5)

The air-cleaning system in each building simulated stack, duct, and hood configurations commonly used by the AEC. Under normal operation filtered air from the six exhaust hoods would discharge into the horizontal header or plenum duct which is centrally connected to a horizontal exit pipe and stack. Exhaust fans were not included because they might have attenuated predicted external shock pressures to levels below those desired for reentrainment studies. Their effect on pressure reduction, however, can be studied conveniently in the laboratory.

The maximum filtering capacity of each air-cleaning system was predicted to be approximately 4500 cu ft/min, based upon the size of the high-efficiency filters employed. In normal operation maximum air velocities would be about 2000 ft/min in the 20-in.-diameter duct and

Fig. 2.1—Door closure and Dust-Stop filter in control room of chemical plant.

Fig. 2.2—Door closure and Dust-Stop filter in concrete house.

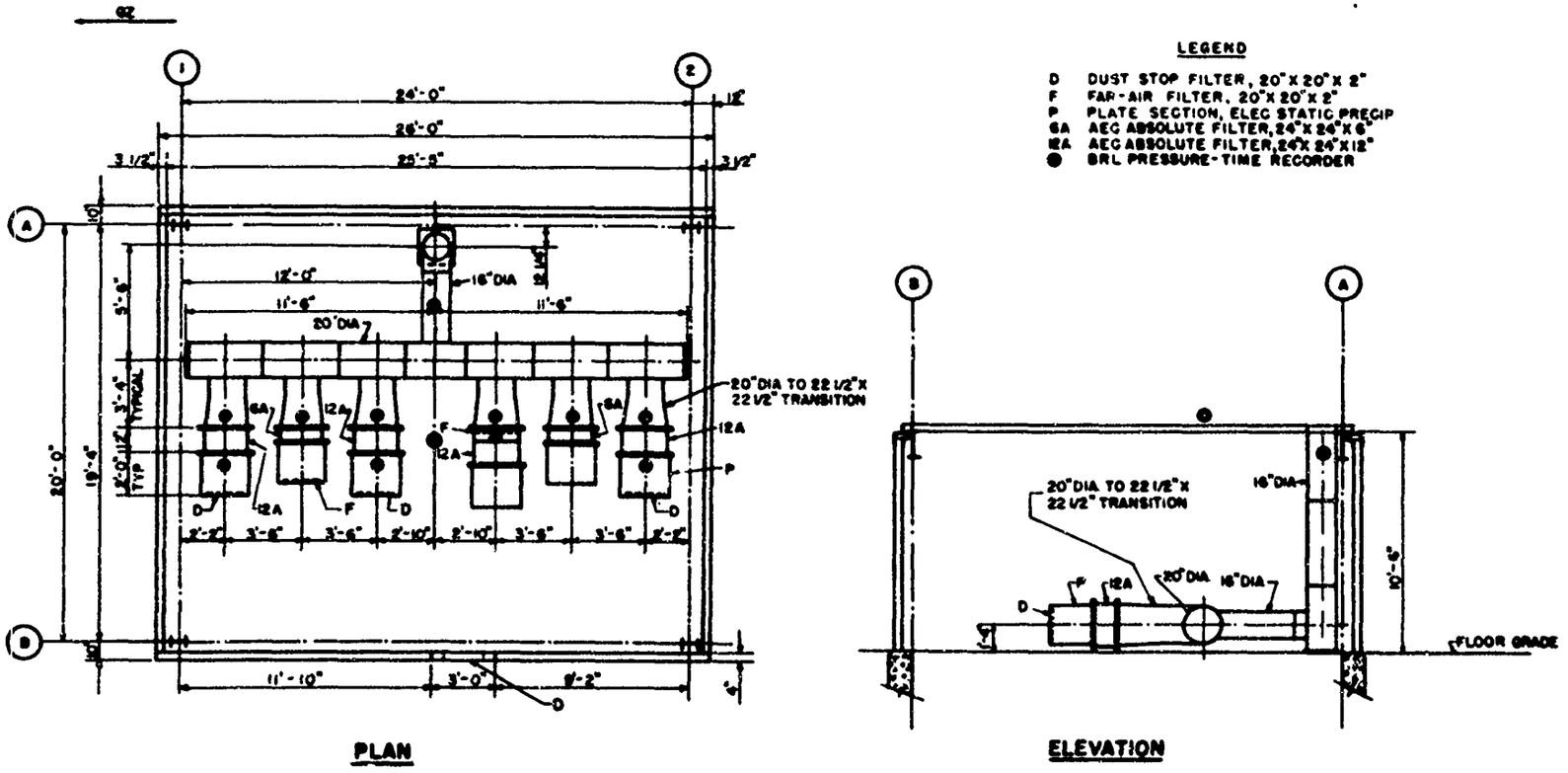

Fig. 2.3—Schematic diagram of ventilation system in chemical plant.

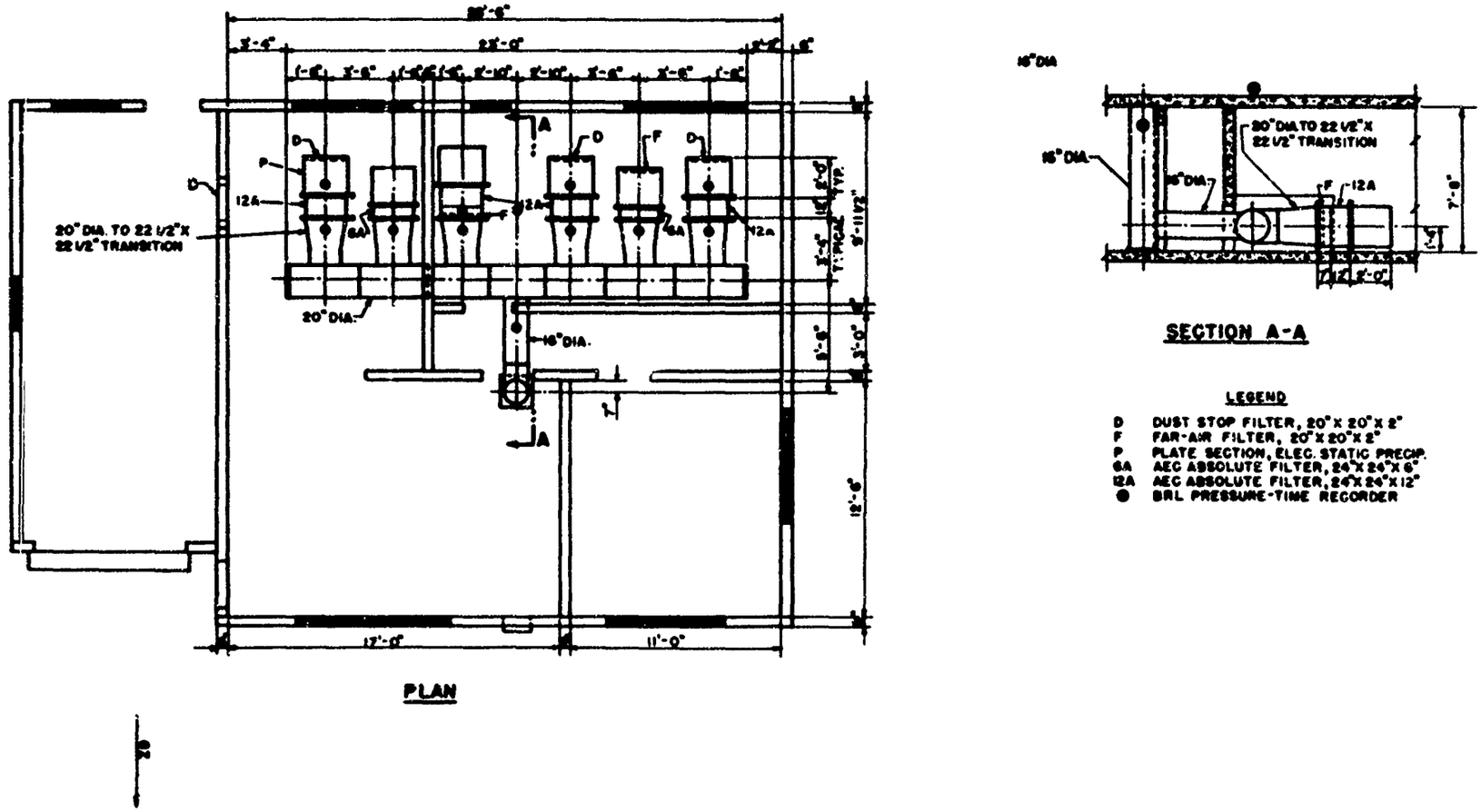

Fig. 2.4—Schematic diagram of ventilation system in concrete house.

Fig. 2.5—Ventilation system in chemical plant. Prestbt.

3200 ft/min in the 16-in.-diameter stack. The exhaust fan would ordinarily be located downstream of the cleaning equipment.

The rectangular wooden duct sections described as hoods represent the type of structure that would be employed in laboratories where filters are located directly behind the bench working area. In production operations air may be filtered immediately behind the exhaust ventilation point and again in a central downstream plenum. Limited space within the test structure did not permit the extension of ductwork beyond the filter hoods. Absence of this ductwork may possibly lead to slightly greater dust reentrainment because of lowered resistance to air flow; however, this factor can be confirmed by comparison with past laboratory studies.

TABLE 2.1— FILTRATION DEVICES AND LOCATIONS IN SIMULATED VENTILATION SYSTEMS

Hood	Prefilter	Final filter	Blow-off afterfilter
1	Dust-Stop* (20 × 20 × 2 in.)	12-in. AEC†	
2	Far-Air‡ (20 × 20 × 2 in.)	6-in. AEC†	
3	Dust-Stop* (20 × 20 × 2 in.)	12-in. AEC†	
4		12-in. AEC†	Far-Air§,¶
5		6-in. AEC†	
6	Dust-Stop** (20 × 20 × 2 in.; electrostatic-precipitator plates)*,**	12-in. AEC*	

*Clean.
†Loaded.
‡Oiled, clean.
§Dry, clean.
¶Not installed in chemical plant.
**Not installed in chemical plant.

A Dust-Stop filter was framed into the door of each structure to simulate supply-air systems normally used in conjunction with exhaust ventilation equipment in large buildings. These filters were placed as far as possible from the stacks so that cross-contamination of supply and exhaust air would be avoided.

Since no supply-air duct systems were used in these tests, a smaller filtration area was chosen to compensate for absence of ductwork pressure loss. In actual practice about three Dust-Stop filters in parallel would be used to match building exhaust capacity.

Supply-air filters in each building were placed in walls subjected to side-on pressure to permit systems comparison.

2.2.2 Filtration Apparatus

Filtration devices placed in each of the six hoods (see Figs. 2.3 and 2.4) are indicated in Table 2.1 according to their positions relative to normal air flow. AEC filters[1] (see Fig. 2.6) referred to are cellulose-asbestos or all-glass media pleated within wooden frames 24 in. square and 6 or 12 in. deep. These filters are designed for high-efficiency collection (>99.9 per cent) of fine (>1 μ in diameter) particles. The 6-in.-deep unit contains about 100 sq ft of filter surface and handles 500 cu ft/min at an initial pressure loss (clean) of 1 in. of water. The 12-in. model has twice the filtration area and operates at 1000 cu ft/min for a 1-in. pressure loss. Under typical operating conditions resistance of a 6-in. AEC filter is approximately doubled when 0.5 to 1 lb of dust (mean diameter, 0.5 μ) is deposited on it. Specific holding capacities depend upon the nature and particle-size characteristics of the dust. Filters may be used for extended periods if sufficient fan capacity is available to handle increased dust loading and if activity levels do not introduce a hazard during filter-replacement operations.

AEC filters used in hoods 1 through 5 for reentrainment studies were loaded in the laboratory under accelerated loading conditions with a reprecipitated calcium carbonate of 1.0 μ (mean size by count). Initial dust holdings averaged about 1.4 lb for a 1000-cu ft/min filter and 0.58 lb for a 500-cu ft/min filter. However, because of spillage losses in transit, precise dust holdings were reestablished by reweighing filters immediately before installation in the ventilation systems.

TABLE 2.2—DUST-HOLDING AND PRESSURE-LOSS CHARACTERISTICS OF AEC FILTERS

Hood	Filter capacity, cu ft/min	Dust load, g	Initial pressure loss, in. water	Pressure-loss increase, in. water
		Concrete House		
1	1000	548	1.16	0.57
2	500	212	0.82	0.33
3	1000*	826	0.93	0.64
4	1000	585	1.21	0.52
5	500*	275	1.10	1.12
		Chemical Plant		
1	1000	744	0.96	0.95
2	500*	357	1.04	0.98
3	1000	575	1.32	0.41
4	1000	554	1.11	0.62
5	500	213	0.92	0.30

*All-glass filter media.

Preshot dust-holding and pressure-loss characteristics of filters installed in hoods 1 through 5 in both structures are summarized in Table 2.2. Pressure-loss increases indicated on the average that the maximum holding capacity was 2.7 lb for a 1000-cu ft/min AEC filter and 1 lb for the 500-cu ft/min size. Variations in loading and resistance characteristics were caused in part by intermittent sloughing-off of the filter cake as a result of mechanical vibration and handling during the loading process. This is more likely to occur under accelerated loading conditions than during actual usage where dust concentrations would ordinarily be much lower.

A clean 12-in. AEC filter was used in hood 6 to attenuate the shock wave. Since any dust dislodged from this filter would interfere with measurement of entrainment losses from electrostatic-precipitator plates immediately upstream, a clean filter was used.

Dust-Stop prefilters (see Fig. 2.7) used in hoods 1, 3, and 6 are standard roughing filters designed to remove coarse (5-μ) particles from the gas stream. Those employed in these tests contain curled 30-μ glass fibers packed within 20- by 20- by 2-in. cardboard frames. The fibers are coated with a thin film of lightweight lubricating oil (SAE 30 weight). Their primary function is to extend the service life of high-efficiency filters.

The Far-Air filter (Fig. 2.8) is an adhesive-coated metal screen, which is normally lubricated by dipping it in oil and then centrifuging or draining to remove the excess. Dimensions and filtration characteristics of this device are about the same as those of the Dust-Stop filters. The Far-Air filter installed in hood 4 was not oiled, however, since its pressure-attenuation characteristics alone were to be studied. Absence of oil eliminated contamination of the adjacent AEC filter which was to be weighed for dust loss.

A collecting-stage section constructed to dimensions of a standard low-voltage electrostatic precipitator (Fig. 2.9) was installed in hood 6. The unit was composed of 34 parallel aluminum plates, $^5/_{16}$ in. apart, aligned vertically and parallel to air flow. Individual plates were 12 in. long, 12 in. high, and $^1/_{32}$ in. thick. All plates were coated with a thin layer of calcium carbonate applied in the laboratory under normal operating voltages (6 kv). Calcium

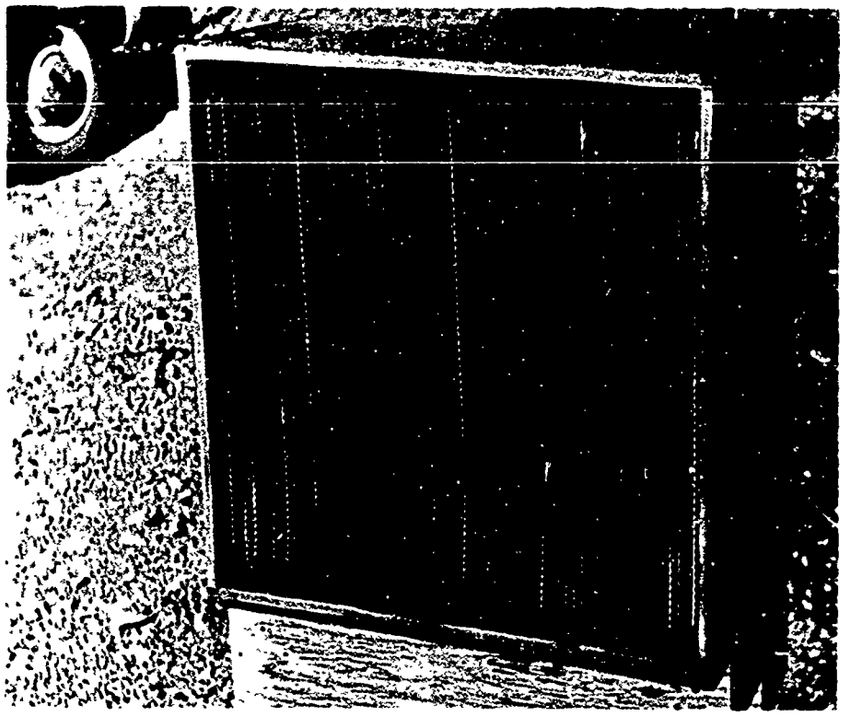

Fig. 2.6—AEC filter.

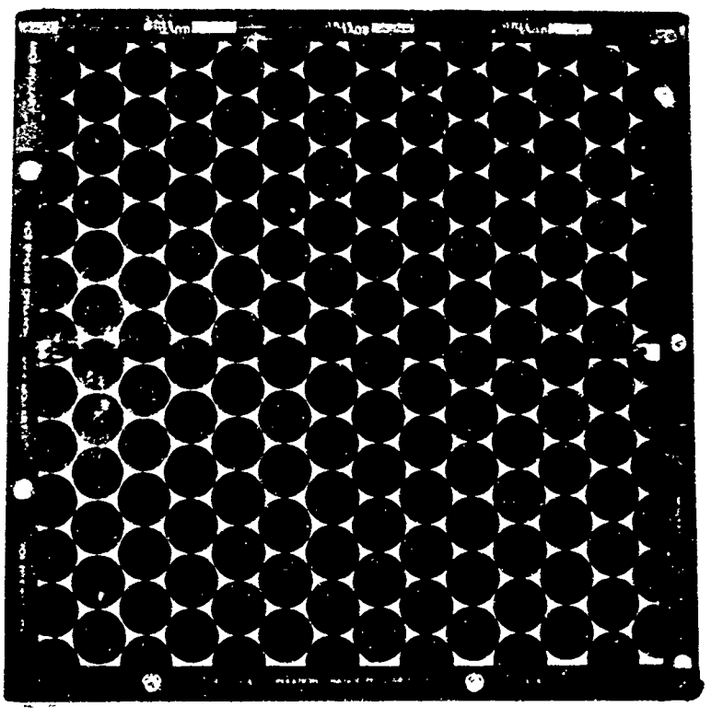

Fig. 2.7—Dust-Stop prefilter.

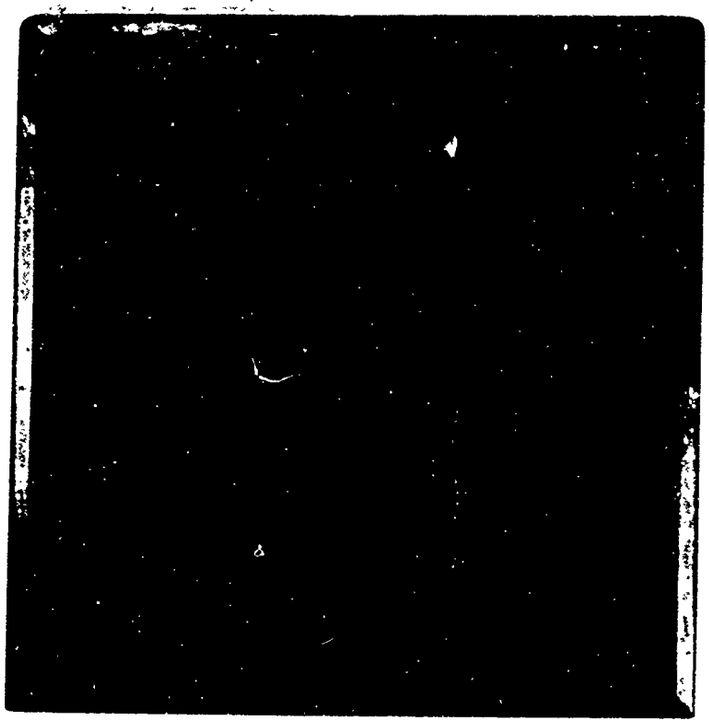

Fig. 2.8—Far-Air filter.

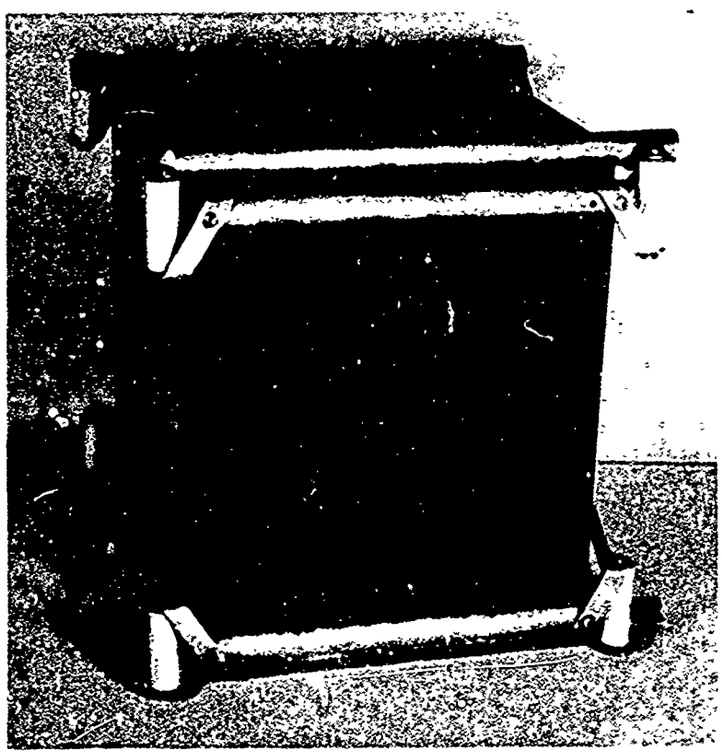

Fig. 2.9—Electrostatic-precipitator collecting stage.

carbonate was selected, since quantities as small as 1 mg can be accurately determined by chemical analysis. Prior to loading, one-half of the plates were lubricated with a thin coating of commercial water-soluble adhesive (TCP). In the field assembly one-half of each unit contained 17 loaded adhesive-coated plates and 17 loaded dry plates. The estimated dust holding per plate was approximately 150 mg; however, final loadings determined in the field for dry plates were about 73 mg per plate.

The amount of dust on the dry plates corresponds approximately to the quantity that would be collected from room air after 3 days of continuous operation and represents about 50 per cent of the holding capacity, assuming a dust concentration of 0.12 mg/m^3 of air and a collection rate of 200 cu ft/min. Under these loading conditions plates would be cleaned on a weekly basis.

2.3 INSTRUMENTATION

2.3.1 Ballistic Research Laboratories Pressure–Time Recorders

Field pressure–time instrumentation was furnished and installed by BRL (WT-1452). The device used for this project was a self-contained unit that records pressure as a function of time. (See Fig. 2.10.) A stylus attached to a compact bellows, composed of two corrugated diaphragms welded together at their edges, traces a continuous record of pressure fluctuations on a rotating glass disk. With proper adjustment, the osmium-tipped stylus produces trace widths of 0.0005 in. on the aluminized glass disk. A battery-powered motor drives the recording disk at a constant speed of 10 rpm. The inner face of the bellows and the recording elements are encased in an airtight chamber so that pressure differences are referred to ambient levels. The pressure-sensing element is located on the inner surface of the flange, or baffle plate, attached to the cylindrical case. When side-on pressures are to be measured, this flange plate is usually set flush with the surface under investigation. The battery motor may be started by a light-sensitive initiator mounted on the flange plate or by conventional timing wire circuitry.

Pressure recorders used in this experiment were available in two ranges, 0 to 5 psi and 0 to 1 psi. Both sizes operate effectively at 100 per cent over maximum rated pressure.

The flanged face of the gauge was bolted to the curved duct surfaces so that the pressure opening on the face of the flange was directly above a 0.5-in.-diameter hole in the duct. The pressure hole and flange were tightly gasketed, and the instrument case was securely braced to supporting pipe sections located directly above.

Gauges were also mounted on plane surfaces of steel and wooden duct. Five-inch-diameter holes were cut in wooden ducts and steel transition sections so that the faceplate of the gauge would be uniformly exposed to duct pressures.

All pressure gauges were connected to a central relay box. Timing signals in both buildings were transmitted by wire simultaneously to actuate the drive motors. Four pressure recorders, located on the roof, stack, horizontal breeching, and in the center of the building, respectively, were operated in the 0- to 5-psi range. The remaining 10 gauges were set for 0- to 1-psi operation. Location of these devices is indicated schematically in Figs. 2.3 and 2.4.

Calibration and preparation of pressure–time records were performed by BRL personnel.

2.3.2 Determination of Filter Weight Losses or Gains

All filters were weighed before and after the test to determine weight losses in the case of AEC filters and weight gains for Dust-Stop and Far-Air prefilters. Several weighings were made to establish equilibrium values since variations in humidity produced significant weight differences with AEC filters (100 to 200 ft^2 of adsorption surface). Blank filter weights were determined before and after the test to correct for moisture gain or loss. Weighings were conducted on a large knife-edge balance which had a working range of approximately 0.5 g to 25 kg.

Dust dislodged from AEC filters and deposited in the hoods between the AEC and Dust-Stop filters was carefully brushed out and weighed on the same balance.

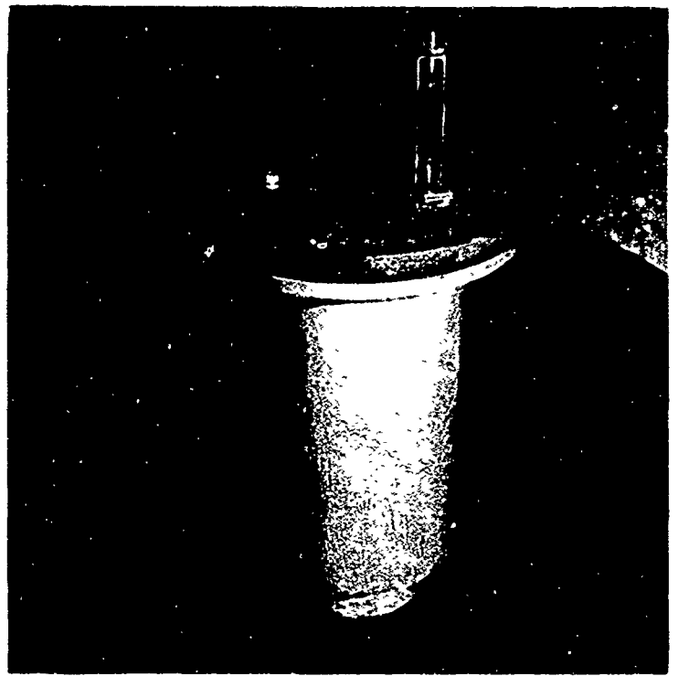

(a)

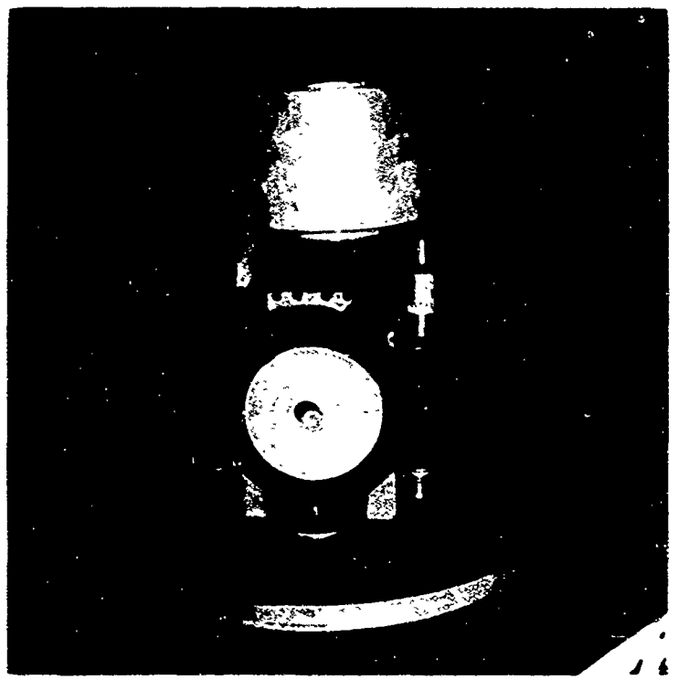

(b)

Fig. 2.10—Ballistic Research Laboratories pressure–time recorder. (a) Complete assembly. (b) Outer case removed.

2.4 EXPERIMENT DESIGN

2.4.1 Pressure–Time Measurements

Identical ventilation and air-cleaning apparatus was installed in both test buildings so that observations could be made under two distinct overpressure conditions. Pressure–time recorders were located on the roof of each building to measure external pressure–time relation in both locations. Pressure–time recorders were also located at the top of the stack, at the midpoint of the horizontal breeching that connected the stack to the 20-in.-diameter plenum duct, and 6 in. in front of (relative to shock-front travel) each of the six hoods. Their function was to indicate the degree of pressure attenuation afforded by a conventionally designed duct system up to the point where the shock front impacted upon air-cleaning equipment.

Pressure–time recorders were placed behind (relative to shock-front travel) the 12-in. AEC filters located in hoods 1, 3, and 6 to determine the attenuation effect of clean and loaded filters. They also served to indicate shock conditions approaching the clean Dust-Stop filters attached to the faces of hoods 1 and 3 and the electrostatic precipitator and Dust-Stop filter installed in hood 6.

These data were needed to allow evaluation of the net shock effect upon filtration apparatus as a result of air entry through the supply port (Dust-Stop filter in door). It is likely that pressure gradients across filters would be reduced significantly if room pressure build-up is significant.

A single pressure–time recorder was mounted between hoods 3 and 4 at an elevation of about 2.5 ft from floor level to measure pressure–time relation within the building proper.

2.4.2 Dust Reentrainment

Loaded AEC filters were placed in hoods 1 through 5 to determine quantity of dust dislodged in terms of (1) the total amount of dust on the filters and thickness of the dust deposit defined by grams deposited initially per square foot of filtration area, (2) the peak pressure and/or total impulse striking the filter, (3) the type and location of auxiliary filtration equipment employed in the system, and (4) no prefilter in the system.

Ordinary weighing methods were used to determine total quantity of dust dislodged from AEC filters, quantity deposited in the hood in front of the prefilter, and amount recovered by the clean prefilters.

Electrostatic-precipitator plates were placed in the unit so that half the collecting stage contained oiled plates and the other half dry plates to allow comparison of dust blow-off under identical conditions. A representative sampling, five samples each of the dry and oiled plates, was made prior to field installation to establish average dust holdings.

Although the collection plates were loaded in a 6-kv field maintained between alternately charged and grounded plates, a power pack was omitted during the field tests. This simulated the worst condition that could occur in the field in event of an electrical power failure. For this reason it is standard practice to back up electrostatic precipitators with stand-by filters to prevent accidental release of contaminants.

2.4.3 Final Installation

It was estimated that at least 8 hr would be required for installation of filtration equipment in both buildings. Since any jarring or rough handling would dislodge dust from filters and therefore invalidate experimental results, this operation was performed after all pressure–time instrumentation had been completed.

Unfortunately, as a result of a sudden change in shot schedule, pressure–time instrumentation could not be completed until 2230 hours on D – 1 day because contractor commitments were behind schedule. The project, therefore, was given special permission to work in the test area until 0245 hours on D-day. Because of limited time the following filter installations were not completed in the chemical-plant control room: (1) Far-Air afterfilter in hood 4 and (2) electrostatic-precipitator plates and Dust-Stop filter in hood 6. This lack of installation precluded the following comparisons: (1) evaluation of the Far-Air filter as a pressure-

attenuation device in two different pressure zones and (2) determination of dust reentrainment from electrostatic-precipitator plates in two different pressure zones.

It is estimated that total equipment installation was about 85 per cent complete in terms of the data sought from these tests.

REFERENCE

1. "Air Cleaning Handbook," U. S. Atomic Energy Commission, Superintendent of Documents, U. S. Government Printing Office, Washington 25, D. C.

Chapter 3

RESULTS

3.1 POSTSHOT CONDITION OF CHEMICAL PLANT AND EQUIPMENT

3.1.1 Building Damage

No significant structural damage to the exterior or interior of the chemical-plant room was observed. A few of the surface cracks on the exterior gypsum wall panels that had been replastered for the current tests were reopened. Gypsum sealing surrounding the stack thimble was dislodged in a few places so that about 20 sq in. of opening existed in the building roof. All temporary window and door closures installed for these tests appeared to be unaffected by the blast. Miscellaneous paper cartons and light equipment left unsecured in the building were essentially undisturbed. Short (2 to 3 ft long) 2- by 4-in. and 4- by 4-in. timbers that were stacked against the outside building wall remained in place.

3.1.2 Exhaust Ventilation and Air-cleaning Equipment

No visible signs of damage or displacement of steel and wood duct systems were detected. All slip joints, steel straps, and bolts were in their original positions. Hood 6 was displaced about 0.5 in. from the steel transition section as a result of improper bolting. With one exception pressure–time recorders appeared to be securely fastened to the ductwork. On hood 4 the recorder located between the Far-Air filter and the AEC filter was accidently loosened during filter installation and was not bolted tightly to the wooden duct.

Preliminary inspection of AEC filters and the Far-Air unit showed no visible signs of damage. Dust-Stop prefilters in hoods 1 and 3 (see Fig. 3.1) were intact with but a slight bowing-out of the center metal supporting strip. The Dust-Stop filter located in the supply-air opening in the entrance door and subjected to side-on pressure was completely destroyed (Fig. 3.2). Most of the debris was found at the base of the stack.

3.1.3 Dust Dislodgement and Degree of Dispersion

Floor areas opposite hoods containing loaded filters were coated with dust. The hoods themselves were completely coated, and significant dust deposits ranging from 20 to 200 g appeared on the bottom sections (Fig. 3.3). Dust-Stop prefilters and the Far-Air filter (Figs. 3.1 and 3.4) were saturated with dust. Dust was deposited on the filter-supporting screens in streamlined wedged-shaped projections, indicating that it had impacted at high velocities. A thin dust film on the outside faces of the filters showed that air flow had reversed during the negative phase of the shock condition.

3.2 POSTSHOT CONDITION OF CONCRETE RESIDENCE

3.2.1 Building and Equipment Damage

No signs of physical damage were noted in the concrete house or in the ventilation and air-cleaning systems. This was expected since the building was in a zone of comparatively

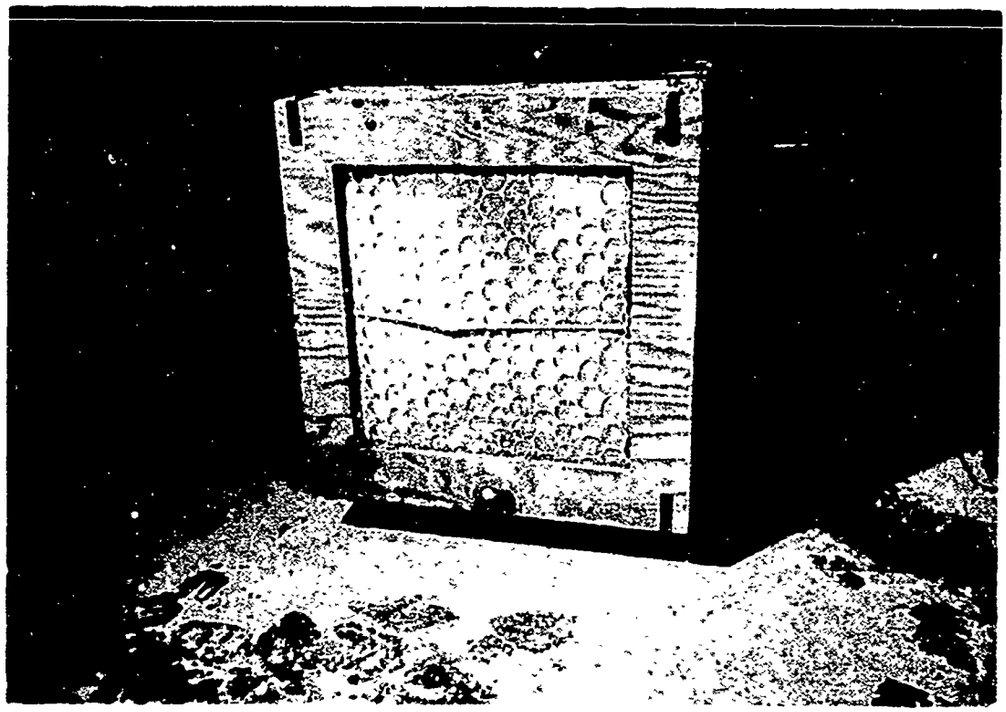

Fig. 3.1—Dust-Stop filter in hood 3 in chemical plant. Postshot.

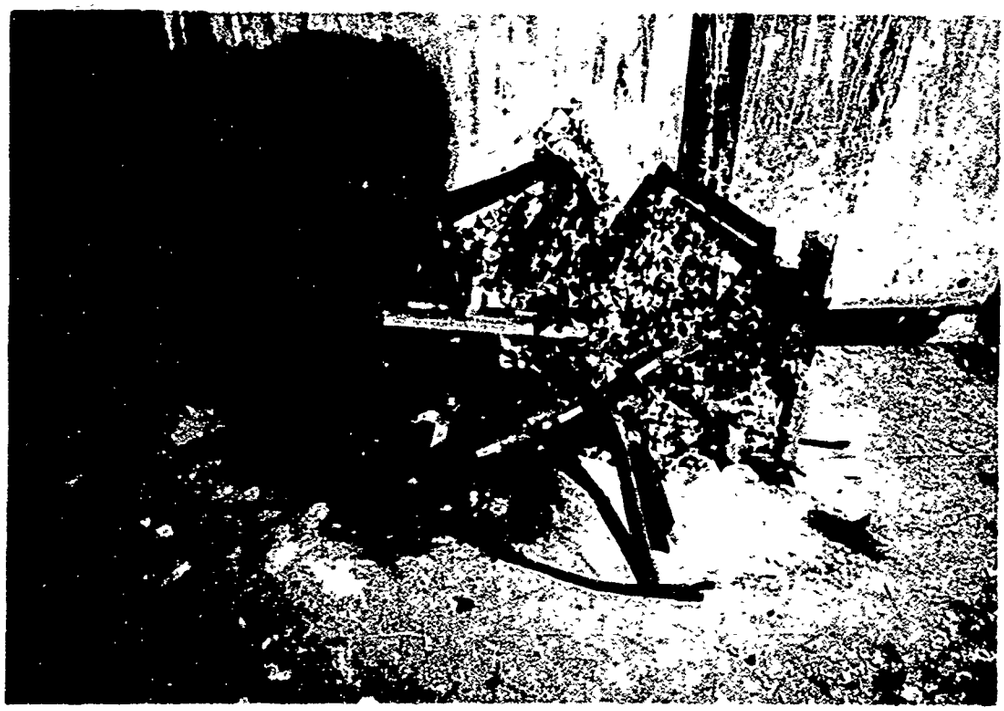

Fig. 3.2—Dust-Stop filter debris in chemical plant. Postshot.

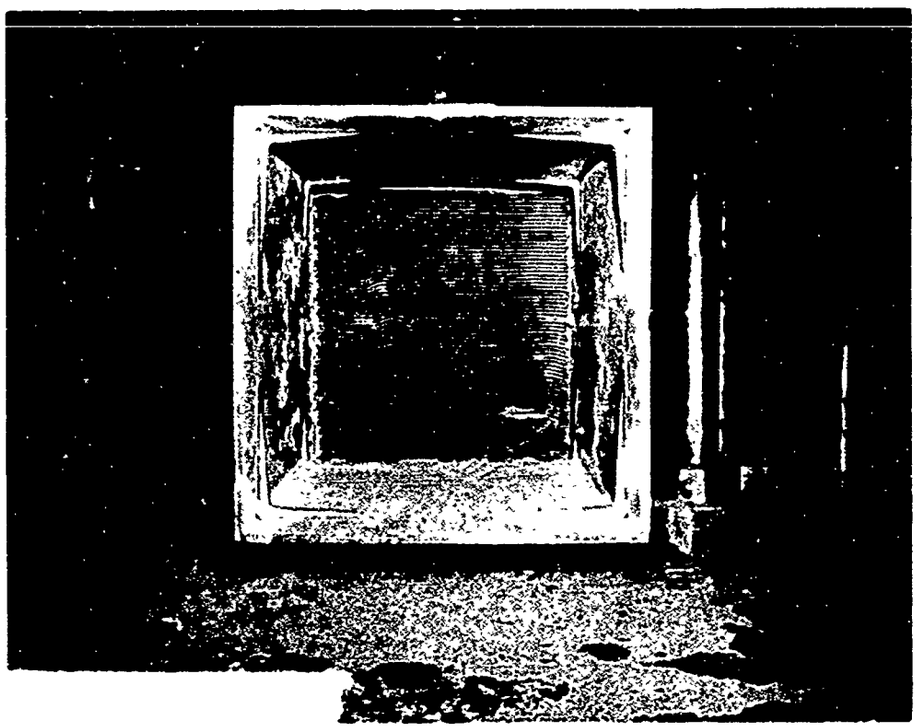

Fig. 3.3—Dust loss from 12-in. AEC filter in hood 4 in chemical plant. Postshot.

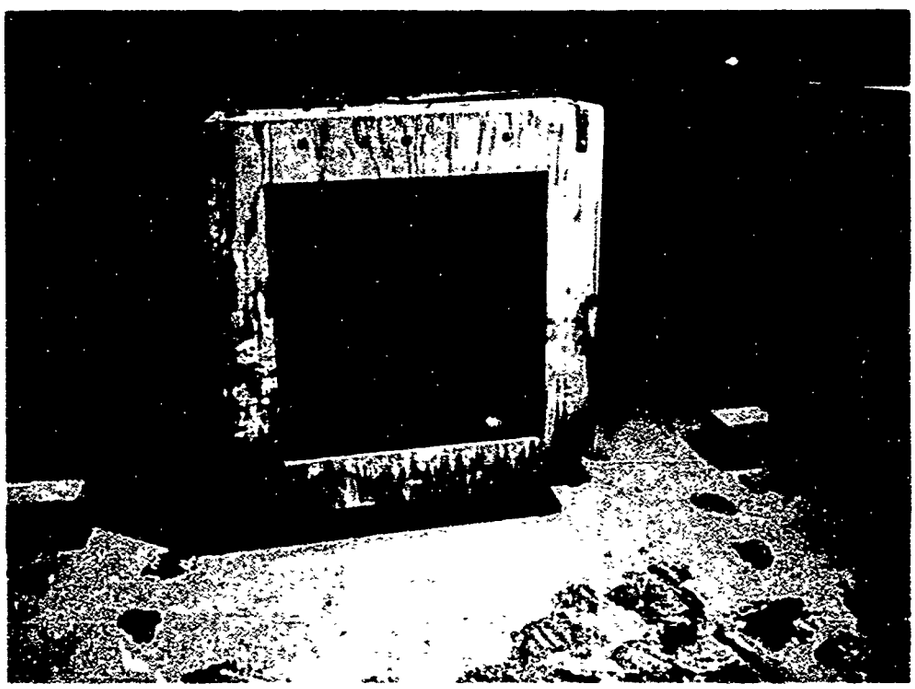

Fig. 3.4—Far-Air filter in hood 2 in chemical plant. Postshot.

low overpressure. However, the supply-air Dust-Stop filter placed in the exit door and subjected to side-on pressure was completely destroyed and blown into the building.

3.2.2 Dust Dislodgement and Degree of Dispersion

In comparison with the chemical plant, no differences were detected in unloading patterns of AEC filters or in dust recovery by prefilters located in hoods 1, 2, 3, and 6. Qualitatively, however, there appeared to be less dust dissemination in this building. Very little dust was deposited in hood 4, which contained a Far-Air filter in front of the loaded AEC filter, indicating that afterfilters might be an effective means of reducing dust dislodgement. The Dust-Stop and Far-Air prefilters in hoods 1, 2, and 3 showed evidence of large dust holdings. A slight bowing-out of the Dust-Stop filter center supporting strip was observed.

Inspection of the electrostatic-precipitator unit in hood 6 indicated negligible removal of dust from the lubricated plates and nearly complete removal from the dry plates. Examination of the interior surface of the Dust-Stop filter in hood 6 confirmed the reentrainment pattern. No significant discoloration could be seen on the side opposite the oiled plates, whereas a pronounced whitening appeared on the metal screening and fibers opposite the dry plates. Examination of this Dust-Stop filter confirmed the fact that there was some back flow through the system during the negative pressure phase since the outer (room) surface showed more discoloration than the interior.

3.3 PRESSURE–TIME RELATIONS

3.3.1 General

A complete photographic record of pressure–time traces relating to this project has been presented in WT-1501 by BRL (Project 39.2).[1] Representative pressure–time traces have been selected to show outside pressure phenomena and those within the ventilation ducts and test buildings. All curves depicted in this report are based upon tabulated pressure–time measurements furnished by BRL. These data were corrected with respect to the original instrument calibrations, and thus they differ slightly from values reported in the interim report of this project[2] and of Project 39.2. Figures 3.5 and 3.6 show pressure–time traces for outside pressures (i.e., building roofs), stack breechings, and building interiors for the chemical-plant control room and the concrete house, respectively. Since pressure–time gauges were oriented with the sensing diaphragms perpendicular to the approaching shock front, static overpressures alone were indicated.

Maximum overpressures of 4.0 and 1.9 psig were recorded within less than 5 msec for outside (roof) pressures in both test locations. A rapid pressure decay, approximately 50 per cent of peak value, was noted during the first 50 to 100 msec, followed by a gradual reduction to ambient pressures at 600 msec outside the chemical plant and 950 msec outside the concrete house. Some minor oscillations were observed for outside pressure curves (Figs. 3.5 and 3.6), which may have been caused by reflections of mechanical vibrations. Only major pulses have been reproduced for traces illustrated in Figs. 3.5 and 3.6.

Instantaneous pressure spikes indicated at stack breechings were approximately 70 per cent of the maximum outside (roof) values. Pressure decay to ambient levels occurred within 10 to 20 msec. During the duct fill period, a steady rise in pressure was modulated by relatively large pressure reflections that led to rather erratic traces. In both test areas reflections were minimal after an elapsed time of 300 to 400 msec. During this time interval maximum duct pressures were about 1.1 and 0.6 psig in the chemical plant and the concrete house, respectively.

Complete failure of Dust-Stop filters that simulated normal supply-air inlets in building side walls provided a second opening for building equilibration with the external environment. Curve 3 of Fig. 3.6 indicates a steady rise in building pressure to a maximum value at 400 msec. A similar curve was estimated for the chemical plant (Fig. 3.5) since the pressure–time gauge showed peak pressure only in this location. Maximum pressures within the chemical plant and the concrete house were about the same as those recorded in the stack breeching

and hood structures over the time interval of 350 to 400 msec. Subsequently, up to approximately 1000 msec, building air vented to the zone of lower pressure existing outside when the major portion of the shock front had passed.

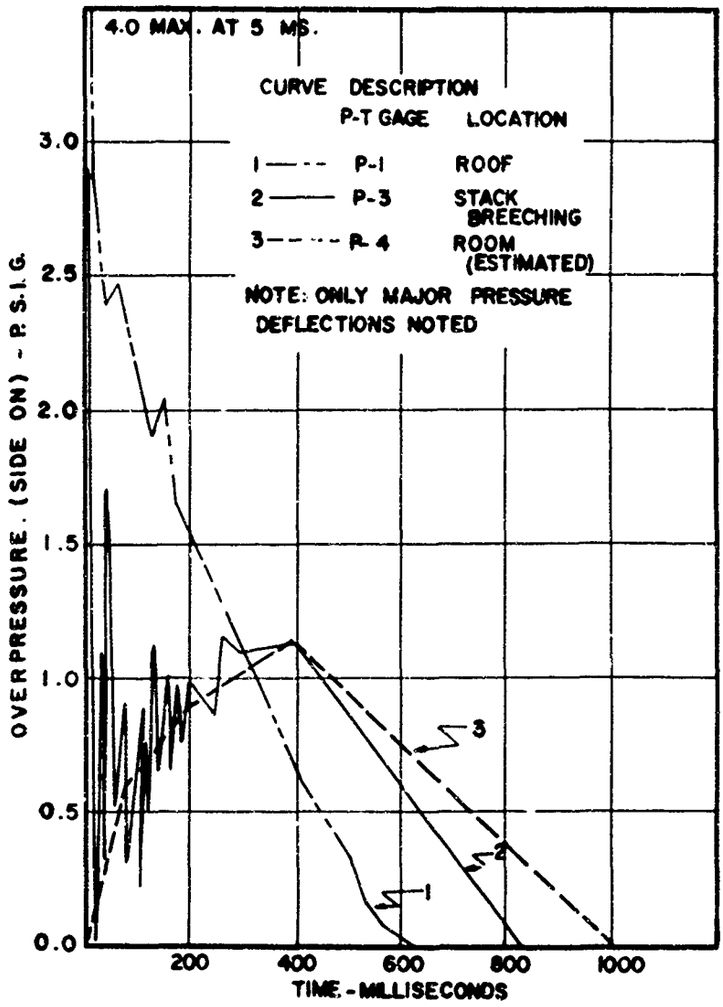

Fig. 3.5 — Pressure - time traces from control room of chemical plant.

Figures 3.7 and 3.8 show typical pressure–time traces upstream and downstream of high-efficiency filters located in hood 3 of the chemical plant and hood 1 of the concrete house, respectively. (Up position refers to the normal clean air outlet of filters facing the oncoming shock-wave). A comparison of curves 1 and 2 in Fig. 3.7 indicates a transient 1.2-psig pressure spike of about 10-msec duration in the zone immediately before the filter. This value is in contrast to a 0.5-psig pressure spike on the downstream side. After 25 to 30 msec, both curves indicate a gradual rise in pressure to a maximum value of 1.1 to 1.2 psig at 375 msec. Oscillations due to reflections were nearly attenuated during this period. Differential pressures across the filters appeared to range from approximately 0.2 psi at 25 msec to zero at 350 msec, with the gradient indicating reverse air flow from the stack. The direction of air flow through the filters reversed after 375 msec as the outside pressure decreased to levels lower than the maximum value attained in the building. Based upon an average resistance of 1.5 in. water at 5 ft/min velocity for partially loaded 1000-cu ft/min AEC filters, it appeared that average and maximum reverse air velocities during the shock phase were 10 and 20 ft/min, respectively. During the venting phase the direction of air flow through filters was in accordance with normal design and was much lower in velocity at an estimated 5 ft/min.

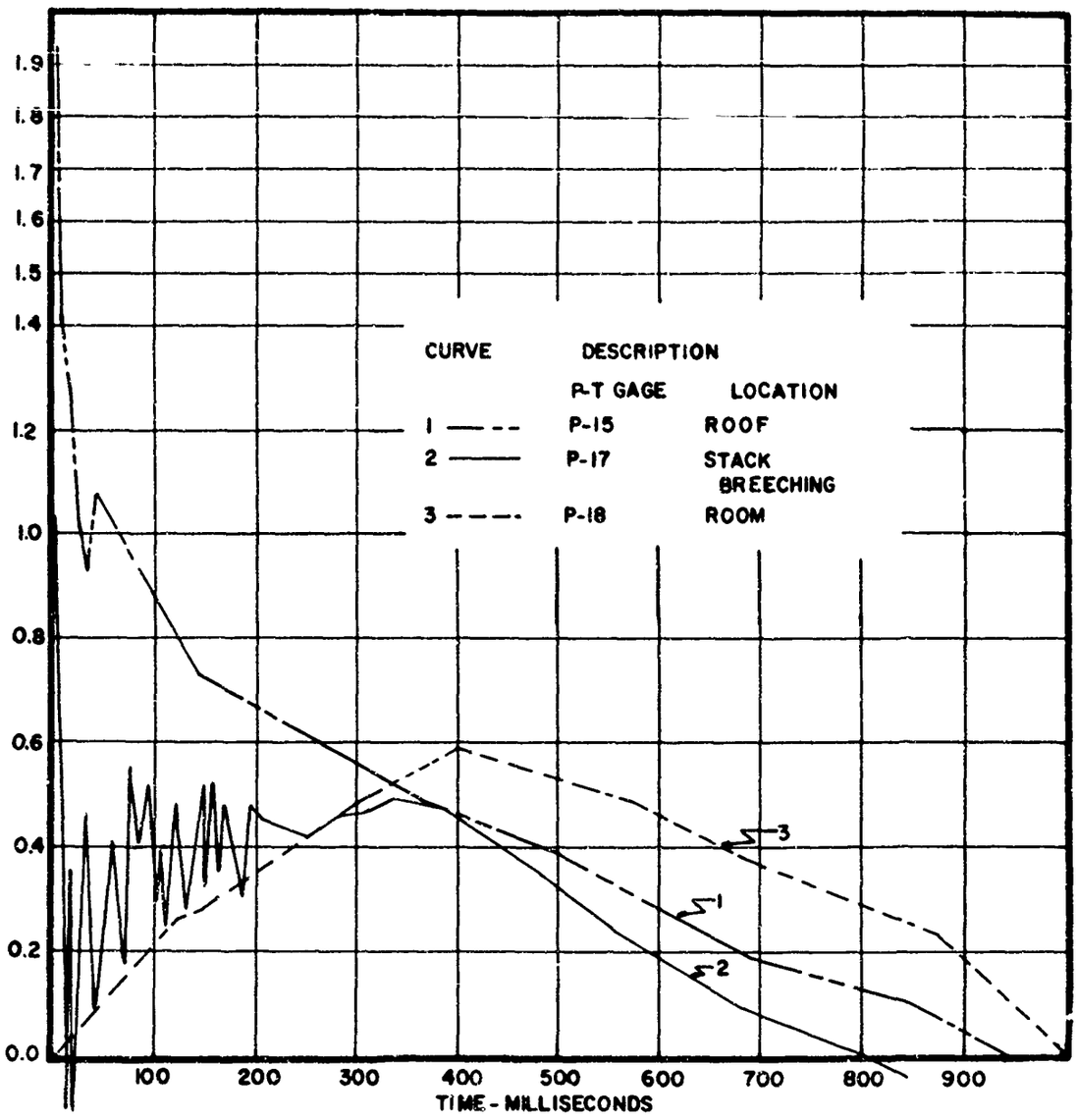

Fig. 3.6—Pressure–time traces from concrete house.

No major differences were detectable among pressure–time curves for the various hoods installed in the chemical plant. In all but one case, a pressure spike ranging in magnitude from 0.9 to 1.3 psig was recorded during the first 20 msec following arrival of the shock. Pressures then decreased rapidly to 0.4 to 0.6 psig, followed by a gradual rise to the building equilibrium pressure of 1.1 to 1.2 psig at 375 msec.

Spike pressures did not correlate with respect to hood position or filter type although both factors would be expected to influence the magnitude of reflected pressures. Average spike pressure, however, was approximately 0.7 that of the peak value observed within any hood system. Some irregularities or inconsistencies in pressure–time traces appeared to have been caused by mechanical vibrations imparted to gauges through the steel ducts. Vibration effects were not evaluated in the field.

Pressure–time traces from the concrete house showed the same characteristics observed in the chemical plant. Initial pressure spikes, however, were relatively small; so, aside from oscillations caused by reflections, the curves maintained a positive slope until the time of maximum fill (350 to 400 msec). The average pressure differential between curves 1 and 2 in

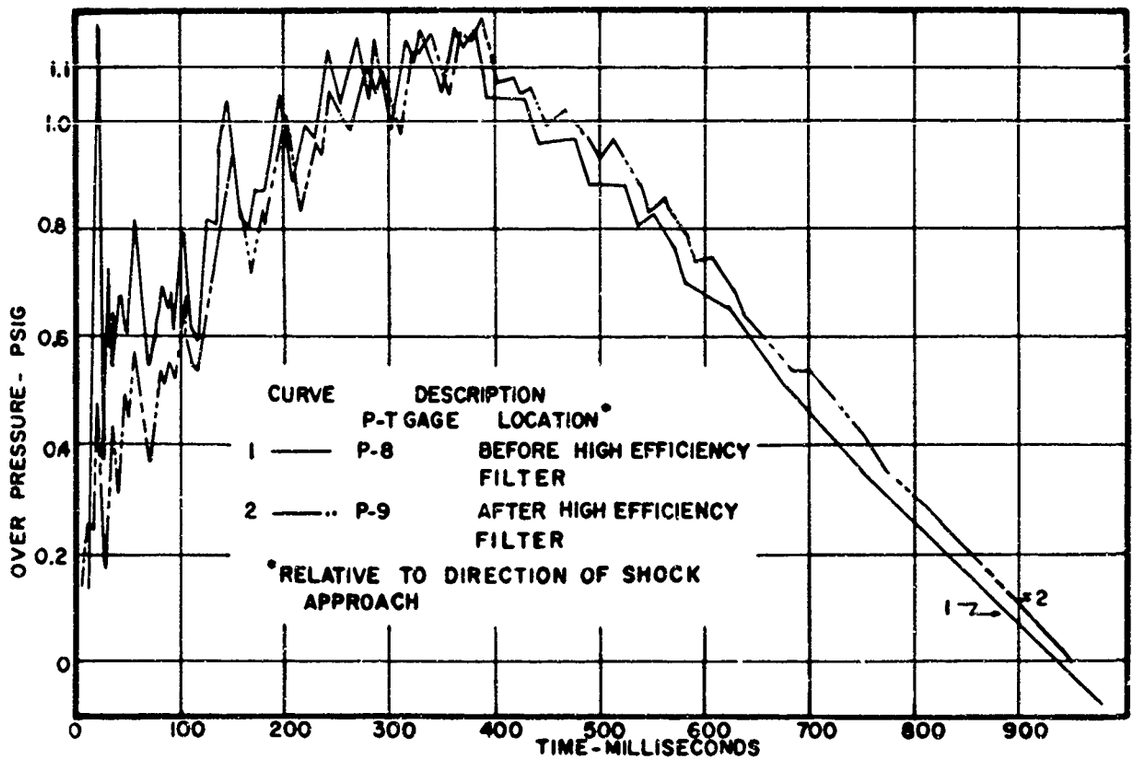

Fig. 3.7 — Typical pressure–time traces upstream (blast side) and downstream of filters in hood 3 in control room of chemical plant.

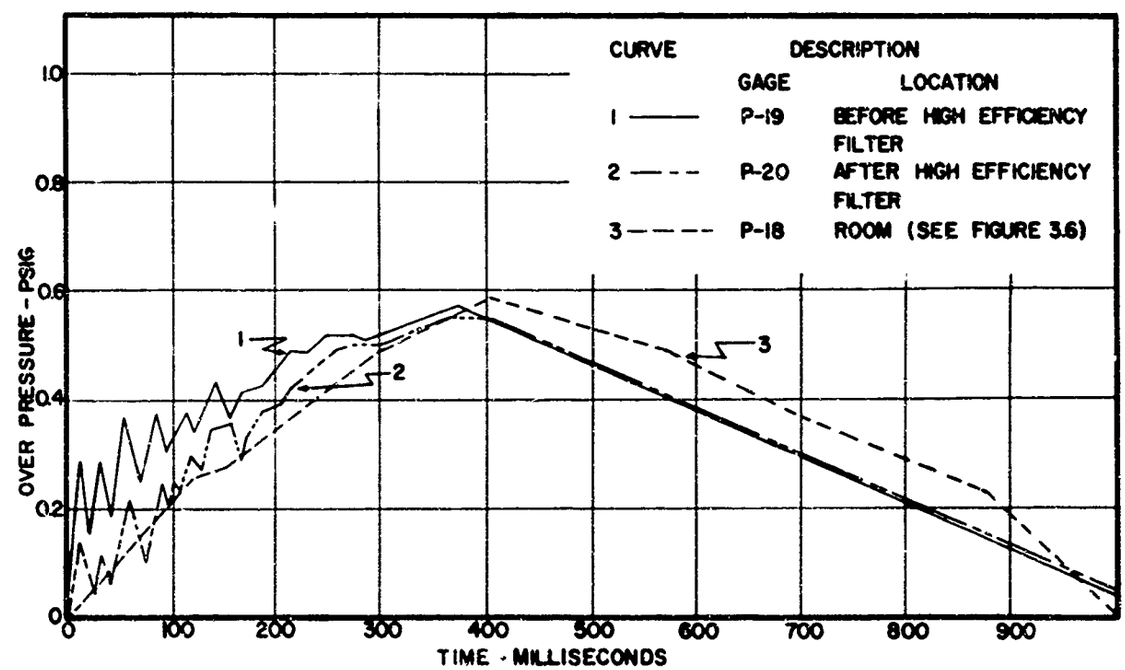

Fig. 3.8 — Typical pressure–time traces upstream (blast side) and downstream of filters in hood 1 in concrete house.

Fig. 3.8 was less than that observed in the chemical plant (0.05 vs. 0.1 psi). During the building venting period, the pressure gradient across the filters also reversed, indicating return to normal air flow through the hood.

TABLE 3.1—PEAK-PRESSURE MEASUREMENTS IN TEST BUILDINGS

	Chemical-plant control room			Concrete house		
Location*	Gauge No.	Peak pressure, psig	Percentage of peak pressure	Gauge No.	Peak pressure, psig	Percentage of peak pressure
Roof	P-1	4.0	100	P-15	1.9	100
Stack	P-2	← No record →		P-16	1.2†	63
Breeching	P-3	2.9	72	P-17	1.3	68
Room	P-4	1.1†	27	P-18	0.59	31
Hood 1U	P-5	1.4†	35	P-19	0.57	30
Hood 1D	P-6	1.2	30	P-20	0.55	29
Hood 2U	P-7	1.2	30	P-21	0.55	29
Hood 3U	P-8	1.2	30	P-22	0.54†	28
Hood 3D	P-9	1.2	30	P-23	0.63	33
Hood 4U‡	P-10	1.0	25	P-24	0.51	27
Hood 4D	P-11	1.4†	35	P-25	0.60	32
Hood 5U	P-12	1.6	40	P-26	0.54	28
Hood 6U	P-13	1.1	27	P-27	0.67	35
Hood 6D	P-14	1.3	32	P-28	0.54	28

*U refers to upstream of AEC filter and D refers to downstream of AEC filter (relative to shock front).
†Peak pressure only; no pressure–time trace.
‡Peak pressure upstream and downstream of Far-Air afterfilter.

3.3.2 Pressure Attenuation in Stack and Duct Systems

Table 3.1 indicates that peak pressures recorded in the stack and breeching of each system were approximately 70 per cent of outside pressures. Pressures in front of the hoods attached to the two branches of the main plenum ducts were about half as large as those in the stack and breeching and about 30 per cent of the outside peak pressure. Upstream hood pressures varied from 1.0 to 1.6 psig for the chemical plant and from 0.5 to 0.8 psig for the concrete house. There did not appear to be any correlation between the magnitude of hood pressures and their points of measurement. No significant differences were noted between peak pressures recorded in front of and behind the AEC filters and the Far-Air filters.

Maximum room pressures in both buildings at equilibrium were about the same as those within the ventilation system (1.1 psig for the chemical plant and 0.6 psig for the concrete house).

3.4 REENTRAINMENT LOSSES FROM AEC FILTERS

3.4.1 General

Table 3.2 summarizes dust losses from AEC filters in both test structures. Filters are identified by hood location and size (6 or 12 in.). Total dust loadings are expressed both by total weight and quantity of dust per square foot of filtration area. Dust losses are described by total weight and percentage of preshot loading. Average dust losses for all AEC filters in the high and low overpressure areas were 73 and 53 per cent, respectively. Hoods 4 and 5 were not included in this average since they did not contain identical apparatus. Peak overpressures determined before loaded dust filters averaged 1.3 and 0.56 psig for the chemical plant and the concrete house, respectively.

TABLE 3.2—DUST LOSSES FROM AIR-CLEANING EQUIPMENT AND RECOVERY BY HOOD AND PREFILTER SYSTEMS

Hood No.	Peak pressure upstream, psi*	AEC filters: Size†	Preshot dust load: Total grams	Preshot dust load: Grams per sq ft surface	Dust loss: Grams	Dust loss: Preshot load, %	Hood dust recovery: Total grams	Hood dust recovery: AEC filter loss, %	Prefilter dust recovery: Type	Prefilter dust recovery: Grams	Prefilter dust recovery: AEC filter loss, %	Prefilter dust recovery: Filter efficiency, %	Dust loss to building, %: Preshot loading	Dust loss to building, %: Dislodged material
Chemical-plant Control Room														
1	1.4	12	744	3.7	557	75	145	26	D‡	109	20	26	41	54
2	1.2	6A	357	3.6	306	86	57	19	F§	90	29	36	45	52
3	1.2	12	575	2.9	331	58	140	42	D	75	23	39	20	35
4	1.0	12	554	2.8	294	53	89	30					37	70
5	1.55	6	213	2.1	155	73	20	13					63	87
6	1.4	No data, equipment not installed												
Concrete House														
1	0.64	12	548	2.7	224	41	77	34	D	73	33	50	14	33
2	0.64	6	212	2.1	110	52	34	31	F	47	43	62	14	26
3	0.54	12A	826	4.1	460	56	169	37	D	116	25	40	21	38
4¶	0.64	12	585	2.9	26	4.5	15	58					2	42
5	0.67	6A	275	2.8	177	64	73	41					38	59
		Electrostatic-precipitator dust load:	Total grams	Grams/plate										
6	0.76	Dry	1.25	0.073	1.18	94	Not measurable		D	Not valid**				
6	0.76	Oiled	3.74	0.22	0	0††								

*Indicates peak pressure immediately in front of AEC filter.

†6 and 12 refer to 500 and 1000 cu ft/min capacity filters, respectively; A indicates all-glass media.

‡D refers to Dust-Stop prefilter.

§F refers to lubricated Far-Air prefilter.

¶Far-Air afterfilter located 9 in. in front of 12-in. AEC filter.

**Weight gain, 3 g, exceeded electrostatic-precipitator weight loss. Actual gain due to backflow of dusty room air.

††Laboratory analyses indicated weight gain. Attributed to backflow of dusty air from room.

3.4.2 Dust Loss vs. Preshot Loading with Pressure Constant

The percentage of dust loss from 6- and 12-in. AEC filters was plotted in Fig. 3.9 as a function of the initial holding, expressed as grams per square foot of filtration surface. An arithmetic scale was selected since it established an additional reference point for curve extrapolation, i.e., zero dust loss with a clean filter. When experimental values were grouped according to building location (and the average approach pressure "seen" by each filter), straight-line approximations appeared to fit the raw data in three out of four cases. All curves, however, eventually become asymptotic to the 100 per cent dust-loss line. According to Fig. 3.9 deviation from linearity appeared to occur when dust losses exceeded 75 per cent of original loadings, as indicated by curve 4.

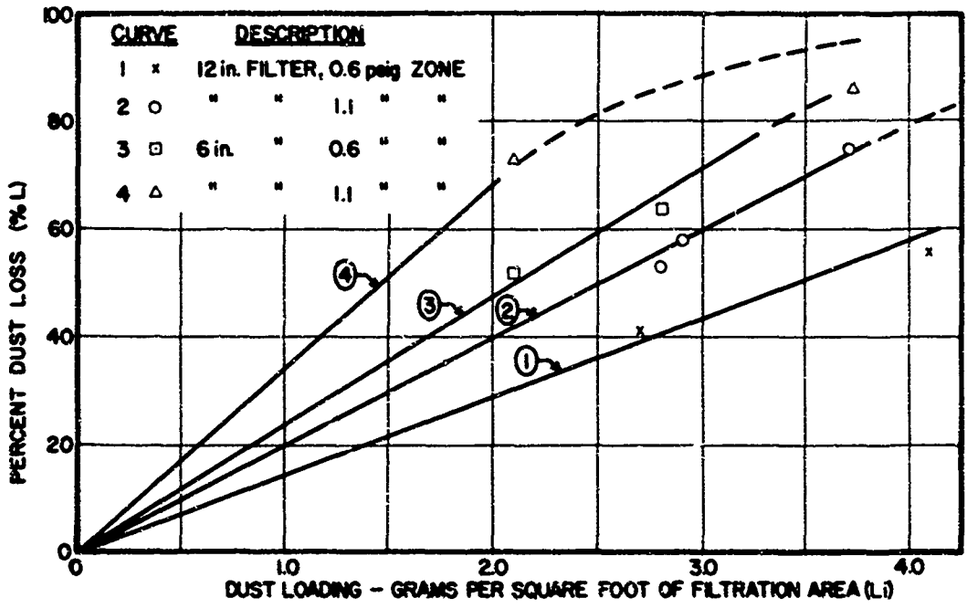

Fig. 3.9—Dust loss from AEC filters vs. initial dust holding.

3.4.3 Dust Loss vs. Pressure Effects with Dust Loading Constant

Preliminary correlations of dust loss with pressure intensity were based upon the only available data, the peak overpressure observed immediately before the filter. Examination of complete pressure–time traces showed that in each test location initial pressure spikes detected by BRL gauges during the first 10 to 20 msec of shock were about 88 and 60 per cent of peak values noted before chemical-plant and concrete-house filters, respectively. Since interior hood structures and positions of outside stacks were similar for both the chemical plant and the concrete house and peak pressures within both systems rose to 31 and 29 per cent of the peak outside pressure, respectively, it appeared that average spike pressures should have been related to outside (or building) peak pressures by the same proportionality factor for both test locations. Therefore it is believed that the use of the peak pressure as an arbitrary means of defining dust loss is justifiable, provided the relation is not extrapolated to shock intensities or duct systems significantly different from those of this study.

By cross-plotting the linear portions of curves 1 through 4 in Fig. 3.9 with respect to constant dust holding and filter size, the percentage of dust loss was found to vary as the 0.41 to 0.46 power of the peak overpressure.

According to pressure–time traces shown in Figs. 3.7 and 3.8, several pressure pulses struck the filters from time zero to approximately 400 msec. Following the initial pressure spike, pulse amplitude appeared to decay in exponential fashion to minimal values at maximum

room fill. Although mechanical vibrations and individual gauge characteristics undoubtedly contributed to the over-all shape of the pressure–time traces, major oscillations were readily identifiable as reflected pressure waves. The characteristic pressure–time traces on the opposite filter faces (relative to shock front travel) followed the same pattern except for spike displacement.

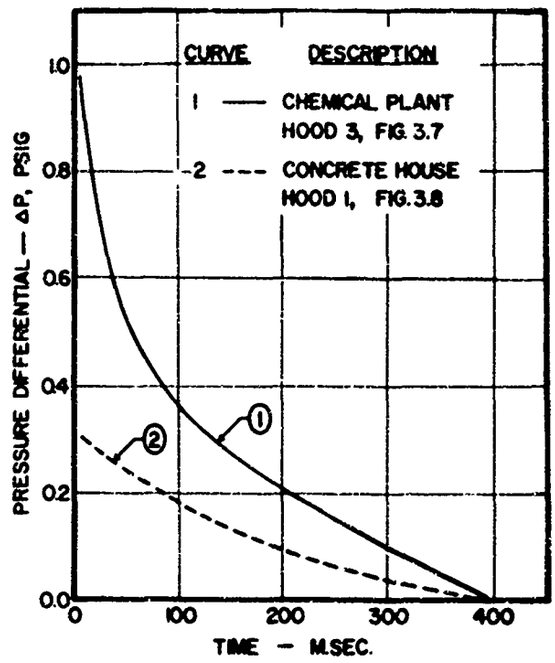

Fig. 3.10—Transient filter pressure differential from time of shock arrival to time of maximum room fill (400 msec).

If the frequency of oscillations is assumed to be the same for both test locations, the difference in area measured between the pressure–time axis for upstream and downstream pressure–time traces is a relative index of total impulse applied to the filter. The instantaneous pressure differential across a filter for a given pressure spike was the difference between upstream spike pressure and the base-line pressure on the downstream filter face. The latter value was closely approximated by the pressure–time trace showing room-fill characteristics. Since gauges were located approximately 3 ft apart, the time interval during which maximum differential values occurred was on the order of 3 msec.

In Fig. 3.10 pressure-spike differentials have been plotted against time for the filter data shown in Figs. 3.7 and 3.8. Total areas under curves 1 or 2 represent true impulses only when pressure decay is a continuous function. It has been assumed here that the integrated value of the product of pressure and time for each individual pulse is directly proportional to, but less than, the value calculated from the smooth curve.

According to graphical integration the total areas under curves 1 and 2 in Fig. 3.10 were 100 and 44 psig-msec, respectively. The ratio of these areas, representing relative impulse "seen" by filters in the chemical plant and the concrete house, was 2.2.

Cross-plotting of the percentage of dust loss at any constant filter loading against the relative impulse imparted to filters in high- and low-pressure locations (see Fig. 3.10, curves 1 and 2) indicated that the percentage of dust loss, %L, was a function of the total relative impulse, Σpt, raised to the 0.4 power. Although essentially the same exponential relation was observed with respect to peak room pressures, examination of complete pressure–time records indicated that the former correlation had limited application. Correlation of dust loss with total impulse is a rational approach provided that the total impulse is treated as an indirect measure of the cumulative effect of several individual pulses.

3.4.4 Dust Loss vs. Filter Size with Pressure and Loading Constant

Figure 3.9 indicates that dust losses were considerably higher for 6-in. AEC filters than those noted for 12-in. units. No distinction could be made between cellulose–asbestos or all-glass media with respect to dust loss. Dust losses at constant pressure and dust loading against filter thickness observed by cross-plotting (see curves 1 through 4 in Fig. 3.9) indicated that the dust loss, L, was related empirically to the filter depth, D, by the following expression: $\%L = kD^{-0.8}$.

3.4.5 Quantitation Dust Loss from AEC Filters

By combining the relations presented in Secs. 3.4.2, 3.4.3, and 3.4.4, the percentage of dust loss from AEC filters was expressed in a single empirical equation

$$\%L = \frac{23.5(\Sigma pt)^{0.4}\, L_i}{D^{0.8}} \qquad (3.1)$$

where Σpt is defined as total relative impulse, the area (in psig-msec) under curves 1 or 2 in Fig. 3.10; L_i is the filter dust holding (in grams per square foot of surface); and D is the filter depth (in inches).

3.5 DUST LOSS FROM ELECTROSTATIC-PRECIPITATOR PLATES

Changes in shot scheduling did not permit installation of electrostatic-precipitator plate sections in the chemical plant. Therefore experimental data indicate only the comparative dust losses between lubricated and dry plate sections in the concrete building. Postshot analyses of lubricated plates in the laboratory indicated a weight gain. This undoubtedly resulted from deposition of dust from general room air during the reverse-flow phase of the shock. Although no quantitative statements can be made with regard to the advantage of adhesives, it may be said that dust loss was significantly reduced. Preshot and postshot weighings of the dust content of dry plate sections indicated 94 per cent reentrainment. Although evidence of considerable dust recovery by the protecting Dust-Stop prefilter was apparent, these data could not be quantitated since the negative phase of the shock caused redeposition of room dust upon the outside filter surface.

3.6 PREFILTER DUST RECOVERY

Examination of dust losses from AEC filters indicated that Dust-Stop and Far-Air prefilters did not have any significant attenuation effect on the quantity of dust dislodged. Table 3.2, however, shows that they prevented 24 and 34 per cent (on the average) of the total amount of dust dislodged from the filters in the chemical plant and the concrete house, respectively, from being disseminated to the room atmosphere.

The percentage of AEC filter dust loss recovered by the prefilters decreased with increasing dust loading. Similarly the collection efficiency of the prefilters based on the quantity of dust reaching them (total dust loss minus total hood recovery) varied inversely with the prefilter holding. No significant differences were noted between the dust-recovery characteristics of the Dust-Stop and Far-Air filters in either test building.

3.7 HOOD DUST RECOVERY

Hood dust recovery in terms of the amount of dust dislodged from AEC filters averaged 26 and 40 per cent for the chemical plant and the concrete house, respectively. No correlation was immediately evident between hood recovery and percentage of dust loss from AEC filters. The presence or absence of prefilters did not seem to influence the quantity of dust retained in the hoods.

3.8 EFFECT OF FAR-AIR AFTERFILTER ON DUST LOSS FROM AEC FILTER

Because of installation difficulties, a Far-Air afterfilter was tested for attenuation effects in the concrete building alone. Results indicated that AEC filter dust loss was reduced greatly by the presence of this filter, 4.5 per cent dust loss compared to an average value of 53 per cent for all other filters in this building.

3.9 TOTAL DUST LOSS TO BUILDINGS

Average values for total dust loss to the buildings (Table 3.2) have been expressed in terms of both the preshot filter holdings and the total dust loss. Based upon preshot loadings, 41 per cent of the reentrained dust from the filters in the chemical plant (4.0-psig area) reached the room atmosphere compared to 22 per cent for the filters in the concrete house (1.9-psig area). Expressed in terms of the total dust dislodgement from the filters in these areas, dust losses were 60 and 39 per cent, respectively. These values furnish, in effect, a measure of the over-all collection efficiency of the combined hood and prefilter systems and indicate 40 and 61 per cent recovery for the filter systems in the chemical plant and the concrete house, respectively.

REFERENCES

1. J. J. Meszaros and J. H. Keefer, Blast Measurements for CETG Projects, Operation Plumbbob Report, WT-1501 (in preparation). (Classified)
2. R. Dennis and C. E. Billings, Blast Effects on an Air-Cleaning System, Operation Plumbbob Report, ITR-1475, November 1957.

Chapter 4

DISCUSSION

A review of complete pressure–time records made available after preparation of ITR-1475, the interim report of this project, indicated that no theoretical basis exists for relating filter damage effects and dust losses to peak pressure values alone. It was noted, however, that peak pressure values reported previously were directly related to the total impulse imparted to filters. Therefore, whereas empirical relations cited in ITR-1475 remain unchanged, final analyses of pressure–time records permitted a more realistic description of the dust dislodgement mechanisms (see Sec. 4.2).

4.1 COMPARISON OF PREDICTED AND OBSERVED PRESSURES

According to a mathematical treatment by BRL[1] the predicted drag pressure experienced by filters in the 3.5-psig zone should have been about 0.037 psi. Drag pressure ($\Delta P_f'$) was calculated by the relation

$$\Delta P_f' = \frac{7}{2}\left(\frac{A_1}{A_f'}\right)^2 \left[\frac{P_1(P_{2,1}^2 - 1)}{6P_{2,1} + 1}\right] \tag{4.1}$$

where $P_{21} = P_2/P_1$
P_1 = atmospheric pressure (12.9 psi)
P_2 = absolute shock pressure (16.4 psi)
A_1 = area of inlet duct (16 in. in diameter)
A_f' = effective filter free area (1880 sq in.)

The effective filter free area A_f' refers to the sum of the face areas immediately preceding each of six hoods. Maximum and average gas velocities calculated from $\Delta P_f'$ were approximately 4000 and 2000 ft/min, respectively, over the period of room fill, 300 to 350 msec. Average gas velocity was estimated from the empirical relation for dynamic pressure decay[2]

$$q(t) = q\left(1 - \frac{t}{t_+}\right)^2 e^{-2t/t_+} \tag{4.2}$$

where q(t) is dynamic pressure at any time t; q is the peak dynamic pressure; and t_+ is the time of positive-pressure duration. In the present application of Eq. 4.2, t_+ was taken as the time of maximum room fill since gas flow through the filter ceased when the pressure gradient became zero.

Since the estimated volume of outside air introduced to the chemical plant from the stack (based upon an average air velocity of 2000 ft/min, a fill time of 350 msec, and an effective filter area of 13 sq ft) was 150 cu ft, the resulting overpressure from this source should have

been 0.35 psi. A similar calculation for the quantity of air entering the building through the 20- by 20-in. supply-air inlet indicated an additional 330 cu ft and a theoretical pressure rise of 0.75 psi. The combined volume, 480 cu ft, in conjunction with the original ambient volume, 5500 cu ft, should have produced a maximum pressure of 14 psi within the building (1.1 psig). Since 1.1 psi was the observed value for maximum overpressure, it appears that the formula suggested by BRL (Eq. 4.1) is applicable to field test conditions.

The average air flow rate through the duct cross section (2.18 sq ft) adjacent to an AEC filter was 4400 cu ft/min according to velocities derived from Eqs. 4.1 and 4.2.

The corresponding interstitial velocity for a 12-in. AEC filter with a total surface area of about 200 sq ft reduces to values on the order of 20 ft/min. Similar filtration velocities were calculated from observed instantaneous pressure differentials across the filter.

Preshot information from BRL[1] also predicted a maximum side-on pressure of 0.5 psig in filter hood locations when the outside shock pressure was 3.7 psig. Instantaneous values of 1.0 psig were also predicted for reflected pressure spikes in the same location. Ballistic Research Laboratories used the following empirical equation to predict pressure levels at the filter face

$$P_2 = \frac{2A_1P_1}{A_1 + A_2} \tag{4.3}$$

where P_1 = outside side-on pressure (psig)
P_2 = side-on pressure at filter face (psig)
A_1 = shock-wave inlet area (sq ft)
A_2 = shock-wave expansion area (sq ft)

The inlet area was that of the 16-in.-diameter stack. It was assumed that the total expansion area was six times that of a 20-in.-diameter duct. Generally, the agreement between predicted and measured values was good, i.e., 1.2 vs. 1.1 psig and 0.56 vs. 0.35 psig for the chemical plant and the concrete house, respectively.

4.2 DAMAGE TO FILTERS

The AEC filters showed no outward indication of having experienced any physical damage at exterior peak pressures of 4.0 and 1.9 psig and hood levels of 1.0 and 0.57 psig. This is consistent with laboratory findings, which showed minor physical damage to occur in the 3.0-psig range (in front of filter).

Dust-Stop filters in supply-air ports were completely destroyed at side-on pressures on the order of 4.0 and 1.9 psig. Previous laboratory tests had indicated partial failures in the 0.75-psig range and complete destruction at 1.5 psig.

Dust-Stop filters used as prefilters in hoods 1, 3, and 6 of each building displayed minor damage, i.e., a slight bending of the supporting metal strips. Since peak pressures immediately in front of these filters averaged 1.0 psig in the chemical plant and 0.57 psig in the concrete house, the complete and partial failure conditions were in general agreement with laboratory tests. However, total pressure differentials across the filters tested in the field were less than the pressures indicated at the impaction faces of the filters because of the partial equilibration made possible by the supply-air openings. Algebraic combination of pressures on either side of the Dust-Stop filters indicated that net pressures in the chemical plant ranged from 0.3 to 0.8 psi. A similar treatment of the filters in the concrete house indicated net shock pressures in the range of 0.1 to 0.2 psi.

4.3 DUST LOSSES FROM AEC FILTERS

For purposes of correlation, dust losses from AEC filters were expressed by the empirical relation given as Eq. 3.1, which takes into account the major variables measured during this study. The percentage of dust dislodgement from several AEC filters containing

varying amounts of dust appeared to be a linear function of the dust-cake thickness (which was directly proportional to the grams of dust deposited per unit surface area). A qualitative observation indicates that the natural shearing force tending to loosen the dust cake from the filter surface is a direct function of the mass or thickness of the dust layer and a type of cohesive bond existing at the filter-dust cake interface. Provided the cake is stationary, the entire weight of the cake is transmitted as a shearing force to the interface, which orinarily represents the weakest point in the structure. Therefore a sudden application of identical shock conditions to filters possessing different loadings should dislodge proportionately more dust from heavily loaded filters than from lightly loaded ones. The suggested linear relation between percentage of dust loss and filter loading assumes that shock conditions were identical for the filters involved in establishing the relation.

It was found that laboratory data showed reasonable agreement with field measurements when Eq. 3.1 was used to predict the percentage of dust removal from the last four filters listed in Table 1.1. Predicted and observed percentage of dust losses were, respectively: 98, 98; 20, 32; 99, 84; and 9, 51.

4.3.1 Effect of Filter Size on Dust Loss

It was observed that 6-in. AEC filters (500 cu ft/min capacity) lost proportionately more dust than the 12-in. models (1000 cu ft/min capacity) when compared under identical conditions of pressure and dust-cake thickness. Empirical quantitation showed the percentage of dust loss to vary inversely with the 0.8 power of the filter thickness. Increased unloading from the 6-in. AEC filters was attributed to two factors: (1) the depth of the filter pleats or pockets was only half that of the 12-in. unit (therefore chance of redeposition of dust within the filter was lessened) and (2) the rigidity of the paper pleats was greater in the 6-in. filter owing to reduced pleat depth (therefore flexure in response to shocks would occur more rapidly and at a higher frequency).

Analyses of pressure–time traces provided no data to show whether or not shock patterns differed for 6- and 12-in. filters.

It was noted that on the average the amount of dust recovered in the hoods was (1) directly related to the quantity discharged from the AEC filters, (2) independent of filter size at constant pressure, and (3) inversely related to the shock pressure. This suggested that decreased hood recovery was associated with higher air and dust velocities or a more finely divided dust. Both factors contribute to lower collection efficiency insofar as capture by settling is concerned. However, the collection efficiencies of the prefilters also decreased with increased AEC filter dust loss. Since these devices are primarily inertial collectors that show improved performance at high velocities, it appeared that a decrease in mean particle diameter was the most likely reason for their lowered efficiencies. Ordinarily, these prefilters are less effective as particle size decreases and show poor efficiencies for diameters less than 5 μ.

4.3.2 Relation Between Impulse and Dust Loss

The mechanisms causing dust removal from filtration devices are not necessarily related to the peak pressure. A gradual pressure increase to comparatively high overpressures would cause relatively little dust dislodgement until air velocities through the media reached values on the order of 2000 ft/min. For example, effective fabric cleaning is achieved in Hersey type reverse-jet blow-ring collectors[3] by directing a high/velocity jet, 2000 to 4000 ft/min, against filter fabrics. On the other hand, a sudden shock or series of shocks similar to those applied to a conventional, mechanically shaken fabric bag or screen also causes significant dust removal.

Qualitatively the actual dust-dislodgement process is associated with the energy imparted to the filter by means of a pulse or series of pulses which decrease in amplitude with respect to time. Unfortunately field and laboratory data represent the integrated effect of several pulses and do not permit analyses on the basis of an individual pulse. It appears, however, that treatment of a single pulse would entail measurement of both amplitude and time duration

since there would be some minimum time duration for which the "shocked" objects would not respond. Conversely, recent findings pertaining to the behavior of a fabric dust collector cleaned by intermittent pulses of compressed air[4] indicated that no significant improvement in cleaning effects was detectable when pulse duration was extended beyond 100 msec. The net result is to suggest that application of impulse to define dust loss should be restricted to systems where transient times associated with individual pulses are similar. Since pulse frequency appeared to be related to pressure reflections and hence ductwork geometry, it is conceivable that alterations in system structure could change the number of reflections.

Data correlated with respect to impulse in both laboratory and field blast studies were based upon similar pressure–time trace characteristics insofar as pulse frequency and duration were concerned.

Investigation of shock-wave cleaning techniques by the Air Cleaning Laboratory[5] (an outgrowth of blast-effect studies) indicated that dust removed from mineral wool filters by air blast followed the same trends reported in the current study. Shock intensities ranging from 1.5 to 4.0 psig caused decreases in filter resistance which were proportional to the cube root of the peak pressure. Since pressure–time traces showed similar exponential decay patterns and essentially the same pressure-spike duration, correlation with respect to total relative impulse would be expected. Filter resistance decrease in the shock-cleaning studies was assumed to be directly proportional to dust loss.

4.3.3 Comparison Between Laboratory and Field Tests

Comparison of field data and laboratory tests indicates that shock-tube experiments summarized in Table 1.1 are in fairly good agreement with field results. Although field pressures were not sufficiently high to confirm damage-level pressures for AEC filters, they did indicate that total destruction and minor failure of Dust-Stop filters occurred at approximately the same pressure levels as measured in the laboratory, 1.5 and 0.75 psig.

Extrapolation of dust losses found in the field by means of Eq. 3.1 showed dust losses in general agreement with those determined in the laboratory.

Field pressure ranges and shock durations with respect to AEC type filters again were on the same order as those obtained in laboratory tests, 0.5 to 3 psig and 700 to 900 msec.

Based upon final analyses of all field data, it now appears that future studies on blast effects on air-cleaning equipment are amenable to laboratory shock-tube treatment.

REFERENCES

1. AFSWP Quarterly Progress Report, Shock-tube Facility, Oct. 1, 1957.
2. S. Glasstone (Ed.), "The Effects of Nuclear Weapons," p. 102, Superintendent of Documents, U. S. Government Printing Office, Washington 25, D. C., June 1957.
3. C. E. Billings, M. W. First, R. Dennis, and L. Silverman, Laboratory Performance of Fabric Dust and Fume Collectors, USAEC Report NYO-1590R, Harvard University, January 1961.
4. R. Dennis and L. Silverman, Fabric Filter Cleaning by Intermittent Reverse Air Pulse, ASHRAE J., 44: 43 (March 1962).
5. C. E. Billings, L. Silverman, R. Dennis, and L. H. Levenbaum, Shock Wave Cleaning of Air Filters, J. Air Pollution Control Assn., 10: 318 (1960).

Chapter 5

CONCLUSIONS AND RECOMMENDATIONS

5.1 CONCLUSIONS

The following conclusions are based upon the limited experimental data obtained in this study. General extrapolation to structures differing widely in closure details and in position and size of air-entry ports (exhaust and supply-air openings) does not appear warranted.

1. No apparent damage to AEC filters housed in prototype ventilation systems occurred at outside peak pressure levels less than 4.0 psig.
2. Complete destruction of Dust-Stop filters occurred at pressure levels greater than 2.0 psig. Minor damage occurred at overpressures greater than 0.4 to 1.4 psig.
3. Reentrainment losses from AEC filters housed in two different structures ranged from 53 to 86 per cent of the initial filter holdings in the 4.0-psig area and from 41 to 64 per cent in the 1.9-psig area.
4. Reentrainment losses varied directly with the initial filter dust load.
5. Reentrainment losses from 6-in. AEC filters were significantly higher than those determined for the 12-in. models.
6. Reentrainment of dust from dry electrostatic-precipitator plates in the 1.9-psig area was high, showing greater than 90 per cent loss.
7. Reentrainment losses from adhesive-coated plates, based upon visual inspection, appeared much lower than those from dry plates.
8. Dust-Stop and Far-Air prefilters were effective in collecting dust dislodged from AEC filters. Results averaged 33 per cent recovery in the 4.0-psig area and 50 per cent in the 1.9-psig area.
9. Large percentages of the dust dislodged from AEC filters were deposited in the hoods immediately in front of the filters. Observed values were 26 and 40 per cent in the 4.0- and 1.9-psig areas, respectively.
10. Considerable dust escaped the hood-filter systems and was discharged into the room atmosphere. The observed amounts were 41 per cent of the preshot loading in the 4.0-psig area and 22 per cent in the 1.9-psig area.
11. The use of Far-Air afterfilters as shock attenuators to minimize reentrainment from loaded AEC filters reduced the dust dislodgement by a factor of greater than 10 (4.5 per cent dust loss in comparison to an average value of 53 per cent for other filters in the 1.9-psig area).
12. Experimental results reported for Dust-Stop filters apply equally well to similar low resistance, low strength, mineral fiber prefilters. Data obtained for Far-Air units also apply to similar steel frame, wire screen, heavy-duty prefilters.
13. Stack and ductwork systems normally located downstream of air-cleaning equipment caused significant attenuation in peak shock pressures. For the structures involved in this study approximately 70 per cent attenuation took place.

14. Analyses of test results indicate sufficient similarity to previous laboratory shock-tube tests to verify that laboratory-scale experiments can yield predictable and reliable results for field applications.

5.2 RECOMMENDATIONS

On the basis of the field tests reported here, it is recommended that any future continuation of this project be confined to laboratory shock-tube tests unless unforeseen complications should arise. The tentative laboratory program suggested by these tests should involve the following:

1. Dust losses from AEC filters and other air-cleaning devices should be investigated at lower overpressures than those already investigated to date in either the field or the laboratory.
2. Use of various types of afterfilters as shock-wave attenuation devices should be studied carefully since limited field data showed promising results.
3. Laboratory pressure–time instrumentation should conform to the type used in the field and should include records of pressure–time relations upstream and downstream of the equipment undergoing test.
4. Final assessment of AEC type filter damage should be based on (1) comparative DOP (dioctyl phthalate) smoke-penetration tests before and after shock exposure and (2) comparative resistance to air flow before and after shock tests since visual examination alone is not sufficient to indicate structural failure.